IJCRT.ORG ISSN : 2320-2882

INTERNATIONAL JOURNAL OF CREATIVE RESEARCH THOUGHTS (IJCRT)

An International Open Access, Peer-reviewed, Refereed Journal

Integrating Network Pharmacology And Experimental Studies For Hepatoprotective Effects Of *Cosmostigma Racemosum* Wight Extract

1Adika kumawat, 2 Prof. Aditi Jyotishi, 3 Dr. Karna Khavane
1,2,3 Department of Pharmacology, Dr.Vedprakash Patil Pharmacy Collage Aurangabad

***Abstract*:** Liver diseases remain a significant global health concern, contributing to substantial morbidity and mortality due to factors such as viral infections, alcohol abuse, and exposure to hepatotoxic chemicals. Conventional pharmacotherapies for liver disorders are often limited by adverse effects and incomplete efficacy, underscoring the need for safer and more effective alternatives. Medicinal plants have garnered increasing attention for their hepatoprotective potential, attributed primarily to their diverse phytoconstituents, including flavonoids, alkaloids, phenolics, and terpenoids. This review systematically compiles and critically examines the evidence supporting the hepatoprotective activities of various medicinal plants, highlighting their mechanisms of action—such as antioxidant, anti-inflammatory, membrane-stabilizing, and antifibrotic effects—as demonstrated in preclinical and, in some cases, clinical studies. Among these botanicals, Cosmostigma racemosum (family Asclepiadaceae) remains underexplored despite its traditional use and rich phytochemical profile. No comprehensive pharmacological studies have yet established its hepatoprotective efficacy. Therefore, this review not only synthesizes current knowledge of established hepatoprotective plants but also delineates the rationale for investigating Cosmostigma racemosum as a novel candidate. Future research into this species could reveal promising bioactive compounds capable of mitigating liver injury and enhancing hepatic function. Such investigations are expected to contribute significantly to the development of plant-based hepatoprotective therapeutics with improved safety and efficacy profiles.

Index Terms: Hepatoprotective, Cosmostigma Racemosum , Network Pharmacology , Phytoconstituents

I. INTRODUCTION: Anatomy of the Liver

The liver is a vital, cone-shaped organ situated in the upper right quadrant of the abdominal cavity, positioned just below the diaphragm and above the stomach, right kidney, and intestines. It appears dark reddish-brown in color and typically weighs approximately 1.4 kilograms (3 pounds).

Blood supply to the liver is derived from two primary sources:

- ✓ Hepatic artery, which delivers oxygen-rich blood.
- ✓ Hepatic portal vein, which carries nutrient-rich blood from the gastrointestinal tract.

At any given time, the liver contains approximately 13% (around one pint) of the body's total blood volume. Anatomically, the liver comprises two major lobes, subdivided into eight functional segments. These segments further divide into roughly a thousand smaller units called lobules. Each lobule is associated with tiny ducts that progressively merge into larger ducts, ultimately forming the common

hepatic duct. This duct carries bile produced by hepatocytes (liver cells) to the gallbladder and the duodenum (the initial section of the small intestine) through the common bile duct.

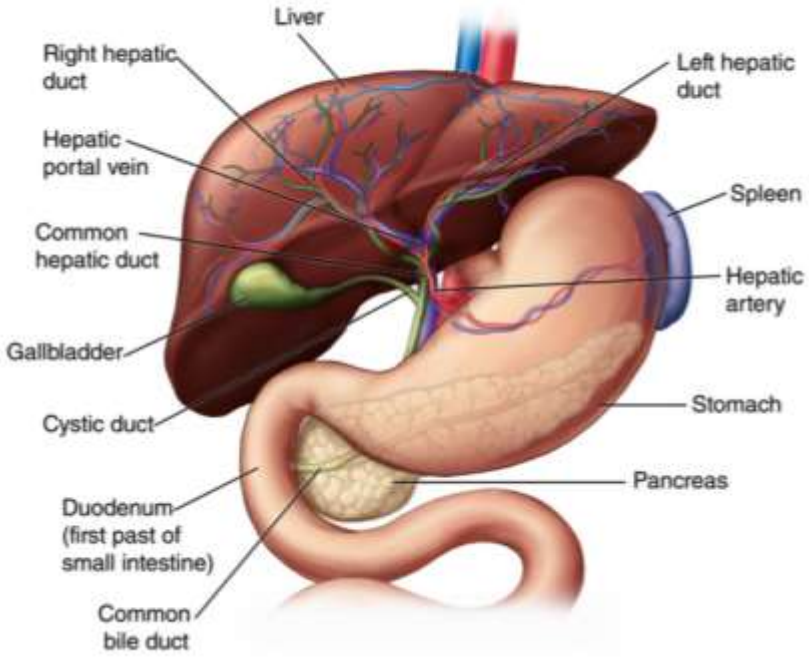

Figure 1: Anatomy of Liver

Functions of the liver

The liver plays a pivotal role in regulating numerous chemical concentrations within the bloodstream and secretes an essential substance known as bile. Bile facilitates the elimination of metabolic wastes and aids the digestion and absorption of fats in the small intestine. All blood exiting the stomach and intestines passes through the liver, where it undergoes meticulous processing. Hepatic cells (hepatocytes) metabolize nutrients, maintain their optimal balance, and convert them into usable forms for various tissues throughout the body. Additionally, the liver metabolizes drugs and other xenobiotics, converting them into safer, less toxic forms suitable for elimination.

Over 500 distinct functions have been attributed to the liver, underscoring its centrality in human physiology. Prominent among these roles include the synthesis of proteins essential for blood plasma, such as albumin and clotting factors, which are crucial for maintaining fluid balance and preventing hemorrhage. The liver synthesizes cholesterol and specialized lipoproteins to transport lipids throughout the body, contributing significantly to lipid metabolism and homeostasis. It serves as a vital energy regulator by converting excess glucose into glycogen for storage and later reconverting glycogen to glucose when energy demands increase.

Furthermore, the liver regulates blood concentrations of amino acids, the fundamental building blocks for protein synthesis. It also facilitates hemoglobin metabolism, effectively recycling iron from senescent red blood cells and storing it for future erythropoiesis. A critical detoxification function involves transforming toxic ammonia, a byproduct of protein catabolism, into less harmful urea, which is subsequently eliminated via renal excretion.

Another vital function is the detoxification and clearance of various drugs, environmental toxins, and other harmful compounds, safeguarding the body against potential toxicity. The liver plays a crucial immunological role by synthesizing immune mediators and by actively removing pathogens from circulation through specialized macrophages known as Kupffer cells. Additionally, hepatic clearance of bilirubin—produced from the breakdown of aged red blood cells—is essential. Disruption in bilirubin metabolism often leads to jaundice, characterized by yellow discoloration of the skin and sclera.

The liver also serves as a major reservoir for fat-soluble vitamins (A, D, E, and K) and trace minerals like copper and zinc, ensuring their adequate availability when dietary intake is compromised. Moreover, it is involved in hormone metabolism, specifically regulating the levels and activities of hormones such as insulin, glucagon, cortisol, and estrogen. Collectively, these myriad functions highlight the indispensable role of the liver in maintaining systemic metabolic balance and physiological health.

II.Material and Methods

Collection and authentication of plant Material

Leaves of *Cosmostigma racemosum* Wight were collected during July–August 2024 from the Sahyadri region, specifically the Bhimashankar area of Pune District, Maharashtra. The plant was taxonomically authenticated by a botanist at Sandip University, Nashik, India. A herbarium specimen was prepared and deposited at the same institution under the voucher number SUN2024/07/03.

Preparation and Storage

The freshly collected plant material was first rinsed with water and subsequently treated with 95% ethanol to inhibit degradation during subsequent storage and drying. The material was then cut into smaller segments and shade-dried until complete moisture removal was achieved. The dried sample was pulverized to a fine powder and sieved through mesh no. 80 for uniformity.

Extraction methodology

A total of 500 g of dried leaf powder was subjected to maceration in a hydroalcoholic solution (70:30) with intermittent stirring at $25 \pm 2°C$ for a duration of three days. The resulting mixture was filtered through a sterilized cotton plug using a Buchner funnel. The solvent was subsequently evaporated to dryness under reduced pressure using a rotary evaporator, yielding 18.65 g of crude hydroalcoholic extract. This extract was utilized for evaluating hepatoprotective activity. The percentage yield of the extract was calculated using the following formula: (Ahmed et al., 2012)

Percentage yield = Weight of Extract / Weight of powdered drug ×100

Pharmacological Investigation

Experimental animals

Male Wistar Albino Rats

Animal identification

Animals used in the study were individually identified using tail marking, while groups and sets were distinguished with colored markers and labeled accordingly. Each label included specific details such as cage number, animal number, and set designation.

Drugs/Chemicals

Paracetamol (PCM)

Quarantine and Acclimatization

Quarantine involves isolating newly received animals from the existing colony to assess their health status and potential microbial load. In this study, newly acquired Wistar albino rats were quarantined for one week to reduce the risk of pathogen transmission to the established population and to ensure physiological and nutritional stabilization prior to experimental use.

Housing

The animals were maintained in a well-ventilated facility under controlled environmental conditions, with temperature and relative humidity maintained at 55–65%. They were housed in spacious polypropylene cages, with paddy husk used as bedding material.

Diet and Water

Animals were provided with a standard pellet diet and access to purified water. Both food and water were available ad libitum, except during designated fasting periods. Bedding was replaced regularly to maintain hygienic conditions.

Drug Administration

Drugs were administered via oral gavage using an oral feeding tube attached to a syringe to ensure accurate dosage delivery. The required quantity of the drug was administered based on the experimental protocol.

Preparation of Dose

The hydroalcoholic extract of *Cosmostigma racemosum* Wight was evaluated at oral dose levels of 100, 200, and 400 mg/kg. Each dose was prepared by accurately weighing the extract and suspending it in 0.3% carboxymethyl cellulose (CMC) solution prepared in distilled water.

Hepatoprotective Model : PCM induced hepatotoxicity

The paracetamol (PCM) induced hepatotoxicity was modied procedure. Rats were divided into six groups consisting of six animals in each group. Group I (Normal control) were administered distilled water containing 0.3% sodium carboxymethyl cellulose (CMC-Na) (1 ml/kg body weight, p.o.) for 7 days. Group II (PCM control) were administered 0.3 % CMC daily, for 7 days and a dose of paracetamol (3 mg/kg, p.o with distilled water) on days 3 and 5 .Group III (Standard treatement) were administered with the standard drug daily, for 7 days, and paracetamol on days 3 and 5, after administration of std drug. Test group animals was administered fruit extract (100, 200 and 400 mg/kg) orally for 7 days. Additionally, 30 min after administration of extract, they received paracetamol on days 3 and 5. On day 7 animals were

anaesthetized and blood was collected, allowed to clot, and serum was separated for assessment of enzyme activity.

The rats were then sacrificed and the livers were carefully dissected, cleaned of excess tissue. Part of the liver tissue was immediately transferred into tris and phosphate buffer for liver tissue parameter in 10% formalin for histopathological investigation.

Table 3 : Distribution of Experimental animals

Groups	Treatment	No of animals	Route
Group 1	Control group	6	Orally
Group 2	Hepatotoxicity induced group	6	Orally
Group 3	Standard drug (Silymarin 25mg/kg)	6	Orally
Group 4	Lower dose of *Cosmostigma racemosum* Wight Extract (100mg/kg)	6	Orally
Group 5	Moderate dose of *Cosmostigma racemosum* Wight Extract (200 mg/kg)	6	Orally
Group 6	Higher dose of *Cosmostigma racemosum* Wight Extract (400 mg/kg)	6	Orally

Description of Distribution of Experimental animals

Experimental animals: Male Wistar Albino Rats

The animals were divided into six experimental groups for the evaluation of the hepatoprotective effect of the Extract. A total of 36 animals were used for this study, with each group consisting of 6 rats. The groups were organized as follows:

Control Group (Group 1):

Rats in this group did not receive any treatment with the Extract or hepatotoxic agents, serving as the baseline or control for comparison.

Hepatotoxicity-Induction Group (Group 2):

Rats in this group were exposed to hepatotoxic agents to induce liver damage but did not receive the Extract.

Standard Treatment Group (Group 3):

Rats in this group were exposed to hepatotoxic agents to induce liver damage and were subsequently treated with a standard dose of the synthetic agent for comparison purpose to investigate potential dose-dependent effects on ameliorating hepatotoxicity.

Hepatotoxicity + Low-Dose Extract Group (Group 4):

Rats in this group were exposed to hepatotoxic agents to induce liver damage and were subsequently treated with a low dose of the Extract to evaluate its potential therapeutic effects on hepatotoxicity.

Hepatotoxicity + Moderate-Dose Extract Group (Group 5):

Rats in this group were exposed to hepatotoxic agents to induce liver damage and were subsequently treated with a moderate dose of the Extract to assess its impact on alleviating liver damage.

Hepatotoxicity + High-Dose Extract Group (Group 6):

Rats in this group were exposed to hepatotoxic agents to induce liver damage and were subsequently treated with a high dose of the Extract to investigate potential dose-dependent effects on ameliorating hepatotoxicity.

Evaluatıon Parameter

Collection of Biological sample: Blood and Serum

At the end of the 14-day treatment period, blood samples were collected retro-orbitally under anesthesia. The animals were then sacrificed using phenobarbital anesthesia. Serum was separated by centrifugation at 3000 rpm for 15 minutes using a centrifuge (Plasto Craft Industries Pvt. Ltd, R4R-V/FA) and subsequently analyzed for various biochemical parameters.

Assessment of hepatoprotective activity

The collected blood samples were allowed to clot, after which serum was separated by centrifugation at 2500 rpm for 15 minutes. The serum was then analyzed in the laboratory for key biochemical parameters, including serum enzymes— aspartate aminotransferase (AST, U/L), alanine aminotransferase (ALT, U/L), alkaline phosphatase (ALP, U/L)—and total bilirubin (mg/dL).

Estimation of Alanine transaminase ALT (SGPT)

Principle

Alanine transaminase (ALT), also referred to as serum glutamate pyruvate transaminase (SGPT), facilitates the reversible transamination between L-alanine and α-ketoglutarate, resulting in the formation of pyruvate and L-glutamate. The generated pyruvate is subsequently reduced to lactate by lactate dehydrogenase (LDH) in the presence of NADH, during which NADH is oxidized to NAD^+. This reaction causes a decline in absorbance at 340 nm, which is directly proportional to ALT enzymatic activity.

Reaction

- L-Alanine + α-Ketoglutarate ⇌ Pyruvate + L-Glutamate (via ALT)
- Pyruvate + NADH + H^+ ⇌ Lactate + NAD^+ (via LDH)

Requirements

Instruments: Autoanalyzer, Micropipettes, Cuvettes, Water bath/incubator (37°C)

Glassware:Test tubes, Volumetric flasks, Beakers

Reagent Contents (Enzymatic UV Kinetic Method)

Reagent Components	Function
Tris buffer (pH 7.4)	Maintains optimal pH
L-Alanine	ALT substrate
α-Ketoglutarate	Co-substrate for ALT
NADH	Coenzyme, reacts with pyruvate
LDH	Catalyzes pyruvate conversion

Preservatives	Ensure reagent stability

Reagents Components:

- *L1 (Enzyme Reagent): Contains buffer, L-alanine, LDH, NADH, α-ketoglutarate*
- *L2 (Starter Reagent): Contains activation agents for initiating the ALT reaction*

Working Reagent Preparation

Commercially available assay kits used directly. The reagents should be mixed thoroughly and maintained at room temperature (25°C) or 37°C, depending on the protocol. For sample-start assays, the working reagent is prepared by combining the entire contents of one bottle of L2 (Starter Reagent) with one bottle of L1 (Enzyme Reagent). This mixture remains stable for up to three weeks when stored at 2–8°C.

Alternatively, smaller quantities of the working reagent can be prepared as needed by mixing four parts of L1 with one part of L2. For individual assays, 0.8 mL of L1 may be combined with 0.2 mL of L2 to obtain 1 mL of working reagent.

Sample Material

The sample material used is serum, free from hemolysis, as hemolyzed samples can interfere with the results. ALT is reported to remain stable in serum for up to 3 days when stored at 2–8°C.

Wavelength and Conditions

- ✓ Wavelength / filter: 340 nm/ filter
- ✓ Temperature : 37°C / 30°C / 25°C
- ✓ Light path: 1 cm

Substrate Start Assay:

Following reagents were pipetted, as per the quantity mentioned in the table below, into clean dry test tubes labeled as Test (T) and serum samples and reagents was added as follows:

Addition Sequence	**(T) 25°C / 30°C**	**(T) 37°C**
Working Reagent (L1)	1.0 mL	1.0 mL
Incubate at the assay temperature for 1 minute and add		
Sample	0.2 mL	0.1 mL

Mix well and read the initial absorbance A and repeat the absorbance reading after every 1, 2, & 3 minutes. Calculate the mean absorbance change per minute (ΔA/ min).

Sample Start Assay:

Following reagents were pipetted, as per the quantity mentioned in the table below, into clean dry test tubes labeled as Test (T) and serum samples and reagents was added as follows:

Addition Sequence	**(T) 25°C / 30°C**	**(T) 37°C**
Enzyme Reagent (L1)	0.8 mL	0.8 mL

Sample	0.2 mL	0.1 mL
Incubate at the assay temperature for 1 minute and add		
Starter Reagent (L2)	0.2 mL	0.2 mL

Mix well and read the initial absorbance A and repeat the absorbance reading after every 1, 2, & 3 minutes. Calculate the mean absorbance change per minute (ΔA/ min).

Calculation :

Substrate / Sample start

SGPT (ALAT) activity in U/L 25 ^{o}C / 30 ^{o}C = ΔA / min. x 952

SGPT (ALAT) activity in U/L 37^{0} C = ΔA / min. x 1746

Temperature Conversion Factor

Assay Temperature	**Desired Reporting Temperature**		
	37°C	**25°C**	**30°C**
25°C	1	1.32	1.82
30°C	0.76	1	1.38
37°C	0.55	0.72	1

Estimation of Aspartate transaminase -AST (SGOT)

Principle

Aspartate transaminase (AST), also known as serum glutamate oxaloacetate transaminase (SGOT), catalyzes the transamination reaction between L-aspartate and α-ketoglutarate, resulting in the formation of oxaloacetate and L-glutamate. The generated oxaloacetate is subsequently reduced to malate by malate dehydrogenase (MDH) in the presence of NADH, which is concurrently oxidized to NAD^{+}. The decline in absorbance at 340 nm, corresponding to the oxidation of NADH, is directly proportional to AST activity in the sample.

Reactions involved

1. L-aspartate + α-ketoglutarate ⇌ oxaloacetate + L-glutamate (via AST)
2. Oxaloacetate + NADH + H^{+} ⇌ malate + NAD^{+} (via MDH)

Requirements

- ✓ Instruments: Autoanalyzer, Micropipettes, Cuvettes, Water bath/incubator (37°C)
- ✓ Glassware:Test tubes, Volumetric flasks, Beakers

Reagent Contents (Enzymatic UV Kinetic Method)

Reagent Components	**Function**
Tris buffer (pH 7.8)	Maintains optimal pH for the reaction
L-Aspartate	Substrate for AST

α-Ketoglutarate	Co-substrate for AST
NADH	Coenzyme, reacts with oxaloacetate
Malate Dehydrogenase (MDH)	Catalyzes reduction of oxaloacetate to malate
Preservatives	Maintain reagent stability and shelf life

Working Reagent Preparation

For the estimation of AST (SGOT) in a sample-start assay, the working reagent is prepared by combining the Enzyme Reagent (L1) with the Starter Reagent (L2). To prepare the full volume, the entire contents of one L2 bottle are mixed with one bottle of L1 to form a uniform solution. This working reagent remains stable for up to three weeks when stored at 2–8°C. For greater flexibility, smaller volumes can be prepared as needed by mixing four parts of L1 with one part of L2. For individual tests, 0.8 mL of L1 may be combined with 0.2 mL of L2 immediately before use, yielding 1.0 mL of working reagent per assay.

Sample Material

The sample material used is serum, free from hemolysis, as hemolyzed samples can interfere with the results. ASAT is reported to remain stable in serum for up to 3 days when stored at 2–8°C.

Wavelength and Conditions

- ✓ Wavelength / filter: 340 nm/ filter
- ✓ Température : 37°C / 30°C / 25°C
- ✓ Light path: 1 cm

Substrate Start Assay:

Following reagents were pipetted, as per the quantity mentioned in the table below, into clean dry test tubes labeled as Test (T) and serum samples and reagents was added as follows**:**

Addition Sequence	**(T) 25°C / 30°C**	**(T) 37°C**
Enzyme Reagent (L1)	0.8 mL	0.8 mL
Sample	0.2 mL	0.1 mL
(Incubate at the assay temperature for 1 minute and then add)		
Starter Reagent (L2)	0.2 mL	0.2 mL

Mix well and read the initial absorbance A and repeat the absorbance reading after every 1, 2, & 3 minutes. Calculate the mean absorbance change per minute (ΔA/ min).

Sample Start Assay:

Following reagents were pipetted, as per the quantity mentioned in the table below, into clean dry test tubes labelled as Test (T) and serum samples and reagents was added as follows:

Addition Sequence	**(T) 25°C / 30°C**	**(T) 37°C**
Working Reagent (L1)	1.0 mL	1.0 mL

(Incubate at the assay temperature for 1 minute and then add)		
Sample	0.2 mL	0.1 mL

Mix well and read the initial absorbance A and repeat the absorbance reading after every 1, 2, & 3 minutes. Calculate the mean absorbance change per minute (ΔA/ min).

Calculations

Substrate/ Sample start

SGOT (ASAT) Activity in U/L 25°C / 30°C = ΔA min. x 952

37°C = ΔA min. x 1746

Temperature Conversion Factor

Assay Temperature	**Desired Reporting Temperature**		
	37°C	**25°C**	**30°C**
25°C	1	1.37	2.08
30°C	0.73	1	1.54
37°C	0.48	0.65	1

Estimation of Alkaline phosphatase (ALP)

Principle

Alkaline phosphatase (ALP) catalyzes the hydrolysis of disodium phenyl phosphate under alkaline pH conditions, resulting in the formation of phenol. The liberated phenol subsequently reacts with 4-aminoantipyrine in the presence of potassium ferricyanide, serving as an oxidizing agent, to form a red-colored quinoneimine complex. The intensity of this color, measured photometrically at approximately 510–520 nm, is directly proportional to the ALP activity in the sample.

Reactions involved

$$\text{Disodium phenyl phosphate} + H_2O \xrightarrow[\text{pH 10.0}]{\text{ALP}} \text{Phenol} + \text{Disodium hydrogen phosphate}$$

$$\text{Phenol} + \text{4-Aminoantipyrine} + K_3Fe(CN)_6 \xrightarrow{\text{ALP}} \text{Red-colored complex}$$

Sample Material

The sample material used is serum, free from hemolysis, as hemolyzed samples can interfere with the results. ALP is reported to remain stable in serum for up to 3 days when stored at 2–8°C.

Wavelength and Conditions

- ✓ Wavelength / filter: 510 nm/ filter
- ✓ Température : 37°C / 30°C / 25°C
- ✓ Light path: 1 cm

Assay:

Following reagents were pipetted, as per the quantity mentioned in the table below, into clean dry test tubes labeled as Blank (B) Standard (S) and Test (T) and serum samples and reagents was added as follows:

Mix well after each addition. Measure the absorbance of the Blank (Abs. B), Standard (Abs. S), Control (Abs. C) and Test (Abs. T) against distilled water.

Addition Sequence	**B (Blank)**	**S (Standard)**	**C (Control)**	**T (Test)**
Distilled Water	1.05 mL	1.00 mL	1.00 mL	1.00 mL
Buffer Reagent (L1)	1.00 mL	1.00 mL	1.00 mL	1.00 mL
Substrate Reagent (L2)	0.10 mL	0.10 mL	0.10 mL	0.10 mL
Mix well and allow to stand at 37°C for 3 minutes, then add:				
Sample	-	-	-	0.05 mL
Phenol Standard (S)	-	0.05 mL	-	
Mix well and allow to stand at 37°C for 15 minutes, then add:				
Colour Reagent (L3)	**1.00 mL**	**1.00 mL**	**1.00 mL**	**1.00 mL**
Sample	-	-	**0.05 mL**	-

Calculassions

Total ALP activity in KA Units = Abs. T – Abs.C / Abs.S –Abs.B

Histopathological studies

For histological evaluation, liver tissues were fixed in 10% phosphate-buffered neutral formalin, followed by dehydration through a graded series of alcohol concentrations (50% to 100%) and embedding in paraffin. Tissue sections of 5 µm thickness were prepared and stained using standard hematoxylin and eosin (H&E) staining protocol. Microscopic examination was performed qualitatively to identify histopathological alterations in the liver tissue.

Network Pharmacology

Screening active phytoconstituents of *Moringa oleifera* leaves

The bioactive phytoconstituents of Cosmostigma species were identified through comprehensive literature review and database mining. A total of 30 phytoconstituents were retrieved, primarily using the Indian Medicinal Plants, Phytochemistry, and Therapeutics (IMPPAT) database (https://cb.imsc.res.in/imppat/), along with reported findings from sources such as Google Scholar, PubMed, and ScienceDirect.

Retrieving phytoconstituents-associated targets

The canonical SMILES of all phytoconstituents were retrieved from the PubChem database (https://pubchem.ncbi.nlm.nih.gov/). The compound-associated target prediction was conducted by entering the canonical SMILES in a total 6 target prediction databases, with the similarity set to 0.5. The databases used include Swiss Target Prediction (http://www.swisstargetprediction.ch/), Similarity ensemble approach (SEA) (https://sea.bkslab.org/), Binding DB (https://www.bindingdb.org/rwd/bind/chemsearch/marvin/FMCT.jsp), Pass online (https://www.way2drug.com/passtargets/), ChEMBL (https://www.ebi.ac.uk/chembl/) and Super PRED target prediction (https://prediction.charite.de/subpages/target_prediction.php).

Retrieving disease-associated targets

Disease-associated genes were identified using keywords such as "hepatotoxicity" and "liver disease." Gene data were retrieved from DisGeNET (https://disgenet.com/), GeneCards (https://www.genecards.org/home), and MalaCards (https://www.malacards.org/) databases. The corresponding UniProt IDs for the retrieved genes were obtained using the UniProt ID Mapping tool (https://www.uniprot.org/id-mapping).

Constructing network and analysing

The Venny tool (https://bioinfogp.cnb.csic.es/tools/venny/) was used to identify overlapping targets between phytoconstituents and disease-associated genes. Protein-compound interaction networks were then constructed using the STRING database (https://string-db.org/) to explore functional associations. Network analysis was further carried out using Cytoscape (version 3.10.3), and the CytoHubba plugin was employed to evaluate network centrality based on degree and other topological ranking algorithms.

Pathway Enrichment Analysis

Gene Ontology (GO) and KEGG pathway enrichment analyses were performed for the top 20 target nodes using the DAVID platform. GO analysis was used to explore the associated biological processes, cellular components, and molecular functions, while KEGG pathway analysis provided insights into the relevant signaling pathways (https://www.genome.jp/kegg/pathway.html).

Molecular docking experiment

Computational molecular docking studies were carried out using the Windows 10 operating system, Intel® Core™ i7-8700 CPU @ 3.20 GHz, and 16 GB RAM, employing the Schrödinger suite 2019-1 via Maestro 11.9 (Schrödinger, LLC, NY, 2019). The interaction pattern and potential binding affinities between the phytoconstituents and core protein were estimated through molecular docking by Mastro Suit.

a) *Ligand and protein preparation*

All ligands were constructed using the Maestro Build Panel and subsequently prepared using LigPrep (Schrödinger), which employed the MMFF94s force field to generate low-energy 3D conformers, molecular geometries, and retain specific chirality. Core protein targets were retrieved based on corresponding gene sequences from RCSB PDB (https://www.rcsb.org/) using selection criteria, including a resolution of ≤ 2.5 Å, Homosapiens origin, and X-ray crystallography and saved in PDB format. Protein is pre-processed to remove water molecules, optimise and minimize to lower energy state for docking by using the protein preparation wizard workflow in the Maestro suite.

b) *Identification of active site*

The site map tool was employed to study the prepared protein's possible binding site by recognizing active ligands. Based on the d-score (nearest to 1) the active site was selected for gride generation.

c) *Molecular docking*

The prepared ligand and protein were docked using glide ligand docking and glide extra precision (XP) mode at active sites identified by the sitemap by considering flexibility

III.Results

Extractive Values

500 gm of plant material were kept for maceration with the hydroalcoholic solution (70% alcohol and 30 % water) (2000 ml) to extract crude extract with occasional stirring at 25 ± 2°C for 3 days.

The extract were then filtered using a Buchner funnel and a sterilised cotton filter. The solvent was completely removed by rotary evaporator and 18.65 g hydroaloholic extract were obtained. These crude extracts were used for investigation of hepatoprotective activity.

Yield of Hydroalcoholic Extract- 3.73 %

Preliminary Phytochemical Investigation

The hydroalcoholic extract of *Cosmostigma racemosum* (Roxb.) Wight leaves underwent standard qualitative phytochemical screening to determine the presence of key secondary metabolites, as summarized in Table 4. The extract tested positive for carbohydrates, flavonoids, tannins, glycosides, and triterpenoids, while alkaloids, proteins, and steroids were not detected. The detection of carbohydrates indicates the presence of fundamental energy-yielding compounds that may enhance the extract's formulation stability. Flavonoids, recognized for their potent antioxidant and free radical scavenging properties, likely contribute to the extract's hepatoprotective and anti-inflammatory potential. Similarly, tannins—polyphenolic compounds with known astringent and antimicrobial properties—suggest additional anti-inflammatory benefits. Glycosides, comprising a sugar moiety bonded to a non-sugar aglycone, were also identified and are well-documented for their broad pharmacological effects, including hepatoprotective, cardioprotective, and antioxidant activities. The presence of triterpenoids, a subclass of terpenes with established anti-inflammatory, hepatoprotective, and anticancer actions, further underscores the therapeutic promise of the extract. Conversely, the absence of alkaloids indicates a lack of nitrogenous bioactive constituents commonly associated with analgesic and central nervous system effects. The non-detection of proteins and steroids suggests the extract lacks macromolecular and steroidal compounds, which are typically linked to hormonal or anabolic activity.

Table 4: Qualitative Chemical Tests of *Cosmostigma racemosum* Wight Leave extract

Chemical Tests	Hydroalcoholic Extract
Alkaloids	-
Carbohydrates	+
Flavonoid	+
Tannin	+

Glycosides	+
Proteins	-
Steroids	-
Triterpenoid	+

Note: (+) Indicates present; (-) indicates absent.

Using different chemical test, preliminary phytochemical investigation of hydroalcoholic extract were performed. The hydroalcoholic extract gave the positive test for Carbohydrates, Flavonoid, Tannin, Glycosides, and Triterpenoid.

Pharmacological Invetigation

Effect of hydroalcoholic extract of *Cosmostigma racemosum* on PCM Induce hepatotoxicity

A) Body Weight

In preclinical studies evaluating hepatotoxicity, body weight variations serve as a useful indicator of potential liver dysfunction. Weight loss may reflect hepatic impairment and is often a sign of concern, potentially linked to metabolic disturbances or reduced nutrient absorption due to liver damage. Conversely, weight gain can also occur in certain cases of liver toxicity, commonly resulting from fluid retention or metabolic dysregulation, though it may not always be directly attributed to liver injury and could arise from unrelated physiological factors. Tracking weight trends over time is crucial, as persistent weight loss or gain may reinforce evidence of hepatic involvement. However, weight changes should be interpreted in conjunction with other indicators of liver toxicity, including altered serum levels of liver enzymes, total bilirubin, and histopathological findings. Additionally, inter-individual differences—such as age, sex, species, and strain—must be accounted for when assessing body weight as a biomarker of liver toxicity in animal models.

The body weight of animals was determined on 1st and 14th day of the study period and these are tabulated in Table 5.

Table 5: Effect of Plant material and Standard drug on body weight of animals

Animal	**Control (Days)**		**PCM induced group (Days)**		**Standard drug (Days)**		**100 mg/kg Extract (Days)**		**200 mg/kg Extract (Days)**		**400 mg/kg Extract (Days)**	
	1	14	1	14	1	14	1	14	1	14	1	14
1.	154	159	158	136	155	161	158	150	157	154	155	149
2.	150	147	160	139	160	152	160	142	156	144	160	153
3.	190	198	165	135	158	150	158	146	169	157	165	168
4.	200	213	158	145	174	162	163	148	154	144	159	151
5.	160	155	160	146	160	151	168	150	163	153	155	158
6.	165	168	163	150	159	149	160	144	160	145	160	149
Means	168.8	171.	160.	141.	160.	154.0	161.	146.	159.	149.	158.	154.

	4	75	64	72	89	7	12	63	75	40	96	52
SD	20.40	26.25	2.80	6.04	6.63	5.77	3.81	3.26	5.49	5.82	3.74	7.33

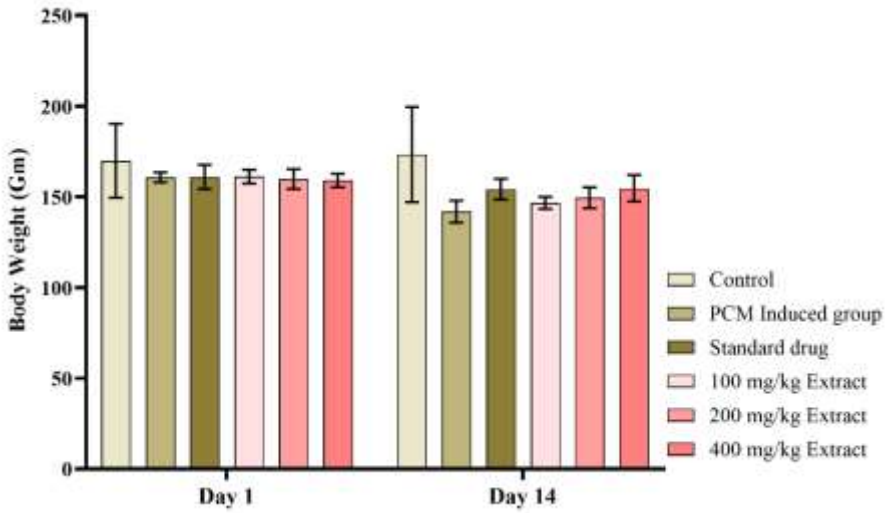

Figure 9: Effect of Plant material and Standard drug on body weight of animals

Body weight was monitored on Day 1 and Day 14 to evaluate the systemic impact of paracetamol-induced hepatotoxicity and the therapeutic efficacy of the hydroalcoholic extract of *Cosmostigma racemosum* Wight. Analysis using two-way repeated measures ANOVA revealed statistically significant effects of treatment (column factor), time (row factor), and their interaction. A highly significant reduction in body weight across all groups between Day 1 and Day 14 was observed ($F(1, 30) = 79.11$, $P < 0.0001$), with treatment groups showing statistically distinct outcomes ($F(5, 30) = 2.90$, $P = 0.0298$). The interaction between time and treatment ($F(5, 30) = 11.18$, $P < 0.0001$) indicates that the pattern of weight change over time was significantly influenced by the treatment regimen. The mean baseline body weight was 161.9 g, which declined to 153.4 g by Day 14, yielding a significant difference of 8.56 g (95% CI: 6.59–10.52), confirming the physiological burden induced by paracetamol toxicity. The PCM control group (Group 2) exhibited the greatest weight loss, highlighting the hepatotoxic effect of PCM. In contrast, the standard-treated group (Group 3) showed a moderate reduction in body weight, indicating partial protection. Test groups receiving the plant extract at 100, 200, and 400 mg/kg (Groups 4, 5, and 6) demonstrated a dose-dependent protective effect. Particularly, the 400 mg/kg group displayed minimal weight loss, closely resembling the normal control group, suggesting that the highest dose of the extract significantly prevented PCM-induced systemic toxicity. These findings provide strong evidence that the hydroalcoholic extract of *Cosmostigma racemosum* possesses significant hepatoprotective and systemic stabilizing activity, as evidenced by preserved body weight under toxic challenge. The statistical significance of all interaction terms further supports the dose-responsive efficacy of the extract in mitigating paracetamol-induced physiological stress in rats.

B) Serum Glutamic Oxaloacetic Transaminase (SGOT)

Serum Glutamic Oxaloacetic Transaminase (SGOT), also known as Aspartate Aminotransferase (AST), is a transaminase enzyme predominantly distributed in the liver, heart, skeletal muscles, kidneys, brain, and pancreas. In preclinical toxicity studies, elevated SGOT levels in serum are a key biochemical indicator of potential hepatocellular injury. Such elevations occur when hepatocytes are compromised or undergo necrosis, leading to the release of intracellular enzymes into circulation. An increase in SGOT levels can signify liver dysfunction induced by the test compound. However, SGOT alone does not provide a comprehensive assessment of hepatic status, as it may also be elevated in response to damage in other organs. Therefore, it must be evaluated alongside additional liver function biomarkers such as serum glutamic pyruvic transaminase (SGPT or ALT), alkaline phosphatase (ALP), total bilirubin, and histopathological findings.

The timing and degree of SGOT elevation offer valuable insights into the nature of hepatic insult. A rapid and marked increase may reflect acute liver injury, while a gradual elevation may be indicative of chronic or progressive liver damage. Moreover, assessing the dose-response relationship is essential to determine the hepatotoxic threshold of the compound under investigation. Interpreting SGOT levels must also consider interspecies variability in liver metabolism and susceptibility to hepatotoxins, which can influence the translational relevance of preclinical findings. Hence, SGOT measurement, when integrated with other clinical and histological endpoints, serves as a vital component of liver toxicity evaluation in preclinical studies.

The SGOT levels of the animals treated with PCM alone and those that were given PCM and Silymarin, *Cosmostigma racemosum* were estimated on Day 14. They are tabulated in Table 6 & 7.

Table 6: Observations of AST (U/ml) of all animal groups

Animal Number	**AST (U/ml)**					
	Group 1	**Group 2**	**Group 3**	**Group 4**	**Group 5**	**Group 6**
1	32.32	169.89	46	144.9	123.7	52.1
2	31.97	168.54	44.43	145.92	122.74	53.62
3	31.57	168.13	46.7	140	134.67	55.67
4	32.56	170.62	45.89	149.71	130.48	53.43
5	34.19	173.26	44.73	155.65	136.52	54.28
6	33.2	169.12	45.48	151.74	125.1	51.41

Table 7: Means Observations of AST (U/ml) of all animal groups

Groups	**Treatment**	**AST (U/ml)** ± SEM
Group 1	Control group	32.62 ± 0.3837
Group 2	PCM induced group	169.91 ± 0.7614
Group 3	Standard drug (Silymarin 25 mg/kg)	45.53 ± 0.345

Group 4	Lower dose of *Cosmostigma racemosum* Extract (100 mg/kg)	147.9 ± 2.2610
Group 5	Moderate dose of *Cosmostigma racemosum* Extract (200 mg/kg)	128.75 ± 2.4032
Group 6	Higher dose of *Cosmostigma racemosum* Extract (400 mg/kg)	53.4 ± 0.6224

Values are expressed as Mean (n=6)

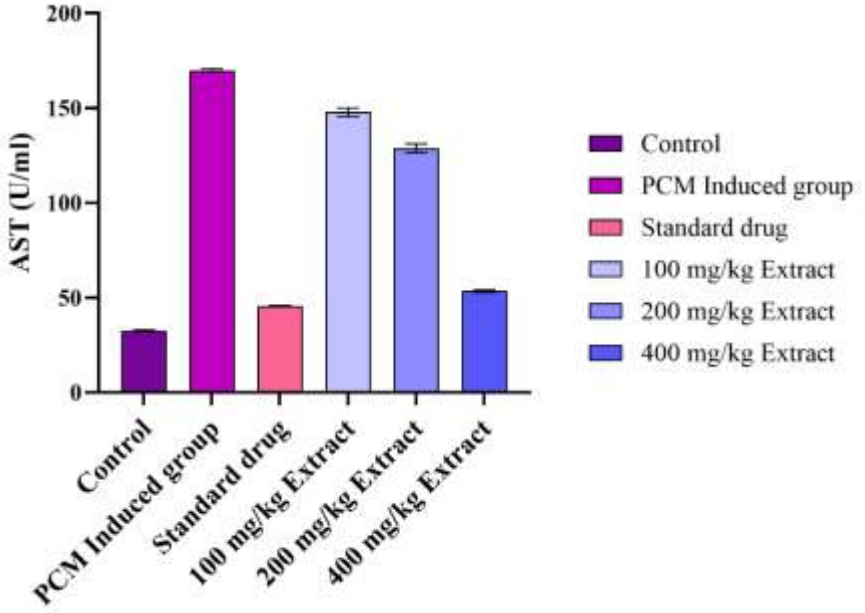

Figure 10: Effect of Plant material and Standard drug on AST Levels (SGOT)

The hepatotoxic effect of paracetamol (PCM) and the protective potential of *Cosmostigma racemosum* Wight extract were evaluated by estimating serum AST (U/ml), a key hepatic marker enzyme. One-way ANOVA revealed a highly significant difference among the treatment groups ($F(5, 30) = 1743$, $P < 0.0001$), indicating that the intervention had a profound impact on AST levels. The R^2 value of 0.9966 confirmed that over 99% of the total variability in AST values was attributable to treatment differences, underscoring the reliability and strength of the findings. Further, Bartlett's test for homogeneity of variances showed a highly significant difference in standard deviations across groups (Bartlett's statistic = 29.56, $P < 0.0001$), confirming heterogeneity in group variances. This variability is expected in pathological versus treated groups, reflecting biological distinctions in response to PCM-induced injury and its modulation by treatments.

In terms of biological interpretation, the PCM control group (Group 2) exhibited the highest AST levels, validating hepatic cellular leakage and necrosis due to oxidative stress and hepatocellular damage. The standard drug group (Group 3) and the extract-treated groups (Groups 4–6) displayed a dose-dependent reduction in AST activity, with the 400 mg/kg extract group (Group 6) showing a marked decline, nearing normal values. This significant restoration of AST towards control levels indicates the hepatocellular

membrane-stabilizing effect and protective efficacy of the extract. To further elucidate the significant differences observed in the ANOVA of serum AST levels, Tukey's multiple comparison test was employed. The results demonstrated that the paracetamol-induced group (Group B) had significantly elevated AST levels compared to all other groups ($P < 0.0001$), confirming severe hepatocellular damage due to PCM administration. The mean difference between the PCM-induced group and the normal control was −137.3 U/L (95% CI: −143.4 to −131.2), indicating a substantial rise in transaminase activity following hepatic insult. Comparisons between the standard drug-treated group (Group E) and the test extract groups (100, 200, and 400 mg/kg; Groups C, D, and F, respectively) revealed important trends. The standard group significantly reduced AST levels compared to the PCM group (mean diff. = −124.4, $P < 0.0001$), validating its hepatoprotective effect. Moreover, the 400 mg/kg extract group (Group F) displayed AST values statistically closer to the control group (mean difference = −20.78, $P < 0.0001$), suggesting that this dose was the most effective in restoring normal hepatic function among the extract-treated groups.

Dose-dependent efficacy of the extract was clearly evident. The 100 mg/kg extract showed a smaller but still significant reduction in AST compared to PCM (mean diff. = −22.02, $P < 0.0001$), while the 200 mg/kg and 400 mg/kg groups exhibited increasingly better protection, with mean differences of −41.16 and −116.5, respectively. The difference between all extract doses was statistically significant ($P < 0.0001$), supporting a clear dose-response relationship. Additionally, a significant difference between the standard group and the 400 mg/kg extract group (*mean diff. = −7.868, $P = 0.0059$) suggested that the highest extract dose may even rival the standard treatment in terms of hepatoprotective efficacy. The compact letter display (A–F) visually clusters the groups based on statistical similarity. The PCM group (A) stood apart from all others, while the 400 mg/kg extract group (D) and standard drug group (E) formed distinct but adjacent clusters, indicating their comparable effectiveness in normalizing AST levels.

These post hoc findings strongly affirm the dose-dependent hepatoprotective effect of *Cosmostigma racemosum* extract against PCM-induced toxicity. The 400 mg/kg dose significantly restored AST levels and exhibited efficacy comparable to that of the standard drug. This suggests potential for the plant extract as a viable therapeutic agent for hepatic injury, especially at higher doses.

C) Serum glutamate pyruvate transaminase (SGPT)

Serum Glutamate Pyruvate Transaminase (SGPT), also known as Alanine Transaminase (ALT), is a liver-specific enzyme widely used as a biomarker for hepatocellular injury. In preclinical studies, elevated SGPT levels serve as a sensitive indicator of liver damage or toxicity. Such elevations often reflect hepatocyte injury resulting from exposure to toxic substances, drug-induced liver injury (DILI), metabolic imbalances, or immune-mediated mechanisms. Monitoring SGPT levels is critical for evaluating the hepatotoxic

potential of investigational compounds. A dose-dependent increase in SGPT levels may suggest a direct correlation between the administered dose and the extent of liver injury. The pattern of SGPT elevation also provides insight into the nature of hepatic damage—acute toxicity is typically associated with a rapid and pronounced rise, whereas chronic injury may present as a sustained elevation over time. To ensure accurate interpretation, SGPT data should be supported by histopathological examination of liver tissues. This is especially important given that interspecies differences in hepatic metabolism and sensitivity to hepatotoxins can influence biomarker expression. Therefore, integrating SGPT analysis with histological findings and additional liver function tests enhances the reliability of hepatotoxicity assessment in preclinical trials.

The SGPT levels of the animals treated with PCM alone and those that were given PCM and Silymarin/ *Cosmostigma racemosum* were estimated on Day 14. They are tabulated in Table 8 & 9.

Table 8: Observations of ALT (U/ml) of all animal groups

Animal Number	**ALT (U/ml)**					
	Group 1	**Group 2**	**Group 3**	**Group 4**	**Group 5**	**Group 6**
1	19.83	182.08	40.07	137.68	76.52	48.25
2	19.93	182.93	42.29	132.37	77.58	49.27
3	20.85	181.22	41.16	136.38	74.66	45.18
4	20.88	186.27	43.29	136.56	78.69	47.16
5	20.85	180.57	39.14	134.52	76.43	46.79
6	19.44	184.31	38.26	132.44	77.79	51.1

Table 9: Mean Observations of ALT (U/ml) of all animal groups

Groups	**Treatment**	**ALT (U/ml)** ± SEM
Group 1	Control group	20.28 ± 0.2606
Group 2	PCM induced group	182.88 ± 0.8615
Group 3	Standard drug (Silymarin 25 mg/kg)	40.66 ± 0.7795
Group 4	Lower dose of *Cosmostigma racemosum* Extract (100 mg/kg)	134.97 ± 0.9168
Group 5	Moderate dose of *Cosmostigma racemosum* Extract (200 mg/kg)	76.93 ± 0.5724
Group 6	Higher dose of *Cosmostigma racemosum* Extract (400 mg/kg)	47.92 ± 0.8445

Values are expressed as Mean (n=6)

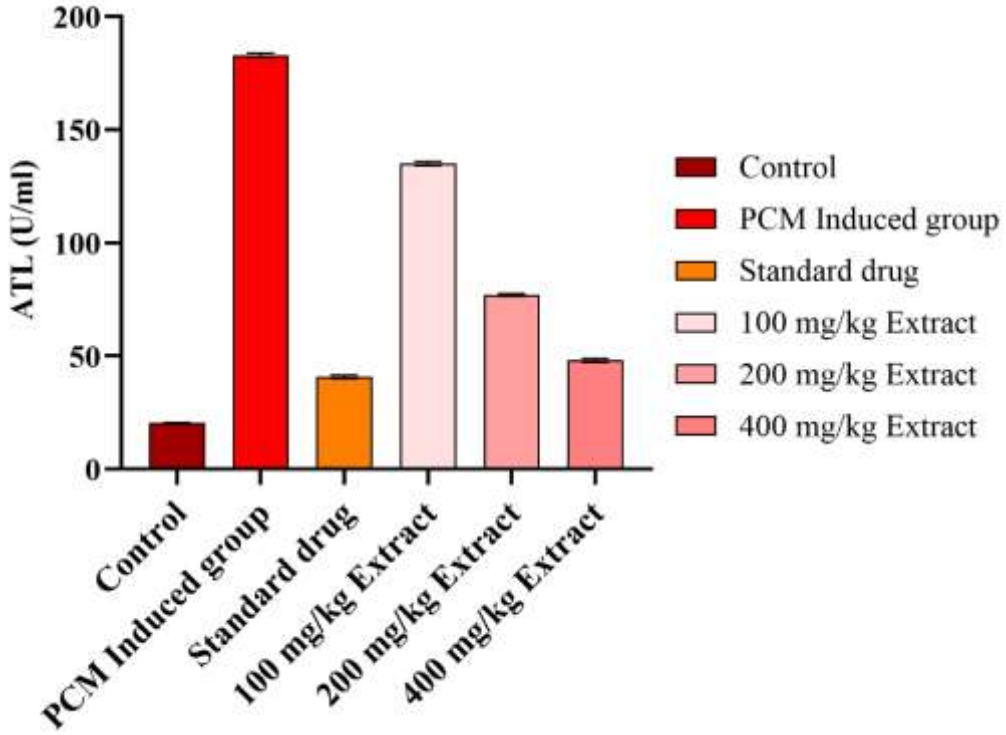

Figure 11: Effect of Plant material and Standard drug on ALT Levels (SGPT)

Serum ALT (U/ml) levels were analyzed as a sensitive marker of hepatocellular integrity and membrane permeability following paracetamol-induced liver injury. One-way ANOVA revealed a highly significant difference among treatment groups ($F(5, 30) = 7152$, $P < 0.0001$), with an exceptionally high R^2 value of 0.9992, indicating that over 99.9% of the total variation in ALT levels was attributable to the treatment effects. This highlights the strong discriminatory power of ALT in assessing liver damage and recovery in this model. Importantly, Bartlett's test for homogeneity of variances yielded a non-significant result ($P = 0.2153$), confirming that the assumption of equal variances was met, and validating the robustness of the ANOVA results. This homogeneity supports reliable inter-group comparisons and reinforces the statistical strength of the observed outcomes.

The results suggest that the PCM-induced group exhibited a dramatic elevation in serum ALT levels, consistent with severe hepatic injury and enzyme leakage into circulation. Conversely, groups treated with the standard drug and plant extract (100, 200, and 400 mg/kg) showed marked reductions in ALT activity, with the 400 mg/kg extract group exhibiting levels closest to the normal control. These findings suggest a dose-dependent hepatoprotective effect of *Cosmostigma racemosum* extract. The extract's ability to lower ALT significantly aligns with its potential to stabilize hepatocyte membranes and reduce enzyme leakage, a hallmark of liver protection. Overall, the ANOVA results affirm that *Cosmostigma racemosum* extract significantly reverses PCM-induced elevations in ALT in a dose-responsive manner, with the 400 mg/kg dose offering hepatoprotective efficacy comparable to the standard treatment. These results corroborate the AST findings and further strengthen the therapeutic potential of this extract in mitigating liver damage.

Following the highly significant ANOVA findings ($F(5, 30) = 7152$, $P < 0.0001$; $R^2 = 0.9992$), Tukey's multiple comparisons test was performed to discern pairwise differences among treatment groups. The PCM-induced group displayed an extremely elevated ALT level (mean = 182.9 U/ml), which was

significantly higher than all other groups ($P < 0.0001$), confirming substantial hepatic injury. The control group, by contrast, had the lowest ALT level (mean = 20.29 U/ml), with a mean difference of –162.6 U/ml when compared to the PCM group, highlighting the toxic impact of paracetamol administration. Treatment with the standard hepatoprotective drug significantly lowered ALT levels (mean = 40.66 U/ml), and the mean difference from the PCM group was 142.2 U/ml ($P < 0.0001$). Notably, the 400 mg/kg extract group achieved ALT levels statistically closer to the control group (mean = 47.92 U/ml), and differed from the standard drug group by only −7.257 U/ml ($P < 0.0001$), indicating comparable hepatoprotective efficacy. A clear dose-response relationship was evident across the extract-treated groups. The 100 mg/kg group showed a substantial reduction in ALT (mean = 135 U/ml) relative to the PCM group, though less than higher doses. The 200 mg/kg dose further improved ALT profiles (mean = 76.93 U/ml), and the 400 mg/kg group offered the most pronounced protection. Each extract dose differed significantly from one another ($P < 0.0001$), reinforcing the presence of a graded therapeutic effect. The compact letter display (A–F) summarized group rankings, placing the PCM group as statistically distinct (A), while the 400 mg/kg extract and standard drug groups (D and E) clustered closely with the control (F), indicating near-normal ALT restoration.

D) Alkaline Phosphatase (ALP)

In preclinical studies evaluating hepatotoxicity, alterations in alkaline phosphatase (ALP) levels are commonly used as a diagnostic marker of liver dysfunction. Elevated ALP levels may indicate hepatobiliary injury, as this enzyme is released into the bloodstream when liver cells are damaged or inflamed. One of the primary hepatic conditions associated with increased ALP is cholestasis—a disruption or reduction in bile flow—which may result from drug toxicity or hepatic inflammation. Drug-induced liver injury (DILI) is a well-recognized cause of ALP elevation, particularly in cases involving bile duct injury or impaired biliary excretion. Biliary obstruction, often linked to toxic metabolites or adverse drug reactions, can further contribute to elevated ALP activity. While metabolic disorders may also influence ALP levels, in the context of liver toxicity assessments, these changes are primarily interpreted in relation to hepatic function. Therefore, monitoring ALP alongside other liver function markers—such as ALT, AST, and bilirubin—provides a more comprehensive evaluation of hepatotoxicity in preclinical models. Elevated ALP should be correlated with histopathological findings to confirm the presence and extent of biliary or hepatic injury.

The ALP levels of the animals treated with PCM alone and those that were given PCM and Silymarin/ *Cosmostigma racemosum* were estimated on Day 14. They are tabulated in Table 10 & 11.

Table 10: Observations of ALP (U/ml) of all animal groups

Animal Number	ALP (U/ml)					
	Group 1	**Group 2**	**Group 3**	**Group 4**	**Group 5**	**Group 6**
1	143.66	210.34	153.59	187.28	174.25	165.86

2	144.45	205.51	151.63	188.48	176.14	164.35
3	140.42	208.71	151.75	186.25	175.08	162.72
4	142.54	210.51	153.68	192.3	177.13	163.71
5	143.62	207.68	152.6	187.27	174.52	162.82
6	143.72	209.52	155.78	190.4	172.97	160.72

Table 11: Mean Observations of ALP (U/ml) of all animal groups

Groups	**Treatment**	**ALP (U/ml) ± SEM**
Group 1	Control group	143.06 ± 0.5854
Group 2	PCM induced group	208.70 ± 0.7714
Group 3	Standard drug (Silymarin 25 mg/kg)	153.16 ± 0.6314
Group 4	Lower dose of *Cosmostigma racemosum* Extract (100 mg/kg)	188.65 ± 0.9301
Group 5	Moderate dose of *Cosmostigma racemosum* Extract (200 mg/kg)	175.00 ± 0.5987
Group 6	Higher dose of *Cosmostigma racemosum* Extract (400 mg/kg)	163.35 ± 0.7076

Values are expressed as Mean (n=6)

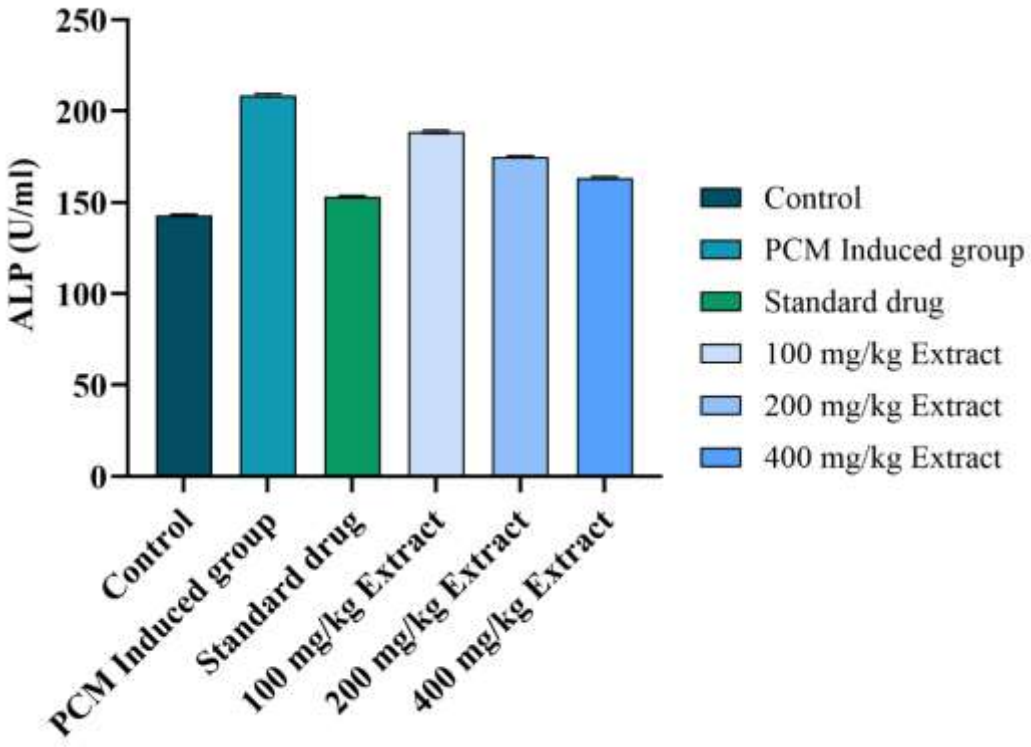

Figure 12: Effect of Plant material and Standard drug on ALP Levels

The one-way ANOVA analysis of serum alkaline phosphatase (ALP) levels revealed a highly significant difference among the six experimental groups ($F(5, 30) = 1137$, $P < 0.0001$), with an exceptionally high R^2 value of 0.9948, indicating that 99.48% of the variability in ALP values is attributable to the treatment groups. This strongly supports the presence of true treatment effects rather than random variation. Homogeneity of variance, a key assumption for ANOVA, was validated by Bartlett's test, which yielded a non-significant result (Bartlett's statistic = 1.547, $P = 0.9076$). This confirmed that the variances were statistically equal across groups, thereby strengthening the reliability of the ANOVA outcome. The significantly elevated ALP levels observed in the PCM-induced hepatotoxic group indicate a severe degree of liver dysfunction. Conversely, extract-treated groups—particularly at 200 mg/kg and 400 mg/kg doses—demonstrated marked restoration of ALP levels toward normal, suggesting potent hepatoprotective efficacy. The low residual variance (MS = 3.061) and high F-ratio confirm the robustness of this statistical finding.

The Tukey's multiple comparison test provided a comprehensive pairwise assessment of ALP levels across all six experimental groups, confirming that each treatment induced a statistically significant alteration in enzyme activity ($P < 0.0001$ for all pairs). The PCM-induced group (Group A) showed the highest ALP levels (mean = 208.7 U/ml), significantly differing from all other groups, which reflects the substantial hepatic damage induced by paracetamol. In contrast, the control group (Group F) exhibited the lowest ALP levels (mean = 143.1 U/ml), as expected in healthy animals. Among the treatment arms, the 100 mg/kg, 200 mg/kg, and 400 mg/kg extract doses (Groups B, C, D) showed a progressive and dose-dependent reduction in ALP levels when compared with the PCM-induced group. The 400 mg/kg group was the most effective among the extract-treated sets, reducing ALP by 45.35 U/ml (mean difference), followed by 33.69 U/ml and 20.05 U/ml for the 200 mg/kg and 100 mg/kg groups, respectively—all comparisons being highly significant ($P < 0.0001$).

The standard drug group (Group E) also demonstrated a strong protective effect with a 55.54 U/ml reduction compared to the PCM group, which was statistically superior to all plant extract groups (e.g., 94.31 U/ml difference vs. 100 mg/kg group, $P < 0.0001$). However, the difference between the standard drug and 400 mg/kg extract group was only 10.19 U/ml, indicating that the highest dose of *Cosmostigma racemosum* extract approaches the efficacy of the standard drug. The compact letter display (A–F) assigned to each group revealed that no overlap existed in any group, suggesting distinct treatment effects across all six cohorts. This separation in letter assignment confirms the robustness of the inter-group differences and supports the dose-responsiveness of the plant extract in reversing PCM-induced hepatic injury.

E) Total bilirubin (TB)

In preclinical studies, total bilirubin serves as a key biochemical marker for assessing liver toxicity. Bilirubin, a breakdown product of hemoglobin, is primarily processed and excreted by the liver. When hepatic function is compromised, as in the case of hepatocellular injury or cholestasis, the liver's ability to clear bilirubin is impaired, leading to its accumulation in the bloodstream. Elevated total bilirubin levels may reflect underlying hepatocellular damage, reduced bile excretion, or both. Conditions such as

cholestasis—marked by impaired bile flow—and drug-induced liver injury (DILI) commonly result in bilirubin elevation. In cases of significant liver dysfunction, elevated bilirubin may lead to jaundice, characterized by yellowing of the skin and sclera. Hepatocytes, the functional units of the liver, release enzymes and metabolites into circulation upon injury, further confirming hepatic compromise. Monitoring changes in total bilirubin levels over time, particularly in relation to the administered dose of a test compound, can help identify dose-dependent hepatotoxic effects. Thus, total bilirubin, when evaluated alongside liver enzymes and histopathological findings, provides valuable insight into the severity and progression of liver injury in preclinical toxicity assessments.

The TB levels of the animals treated with PCM alone and those that were given PCM and Silymarin/ *Cosmostigma racemosum* were estimated on Day 14. They are tabulated in Table 12 & 13.

Table 12: Observations of TB (U/ml) of all animal groups

Animal Number	**TB (U/ml)**					
	Group 1	**Group 2**	**Group 3**	**Group 4**	**Group 5**	**Group 6**
1	0.3147	1.4312	0.3349	0.5989	0.5379	0.3756
2	0.3248	1.3906	0.3553	0.6293	0.5278	0.3857
3	0.3045	1.4007	0.3553	0.609	0.5481	0.3654
4	0.3248	1.4109	0.3451	0.6192	0.5684	0.3756
5	0.3147	1.3906	0.3349	0.6699	0.5887	0.3857
6	0.3147	1.3703	0.3349	0.6293	0.5278	0.406

Table 13: Mean Observations of TB (U/ml) of all animal groups

Groups	**Treatment**	**TB (U/ml)** ± SEM
Group 1	Control group	0.31 ± 0.0031
Group 2	PCM induced group	1.39 ± 0.0084
Group 3	Standard drug (Silymarin 25 mg/kg)	0.34 ± 0.004
Group 4	Lower dose of *Cosmostigma racemosum* Extract (100 mg/kg)	0.62 ± 0.01
Group 5	Moderate dose of *Cosmostigma racemosum* Extract (200 mg/kg)	0.54 ± 0.0099
Group 6	Higher dose of *Cosmostigma racemosum* Extract (400 mg/kg)	0.38 ± 0.0056

Values are expressed as Mean (n=6)

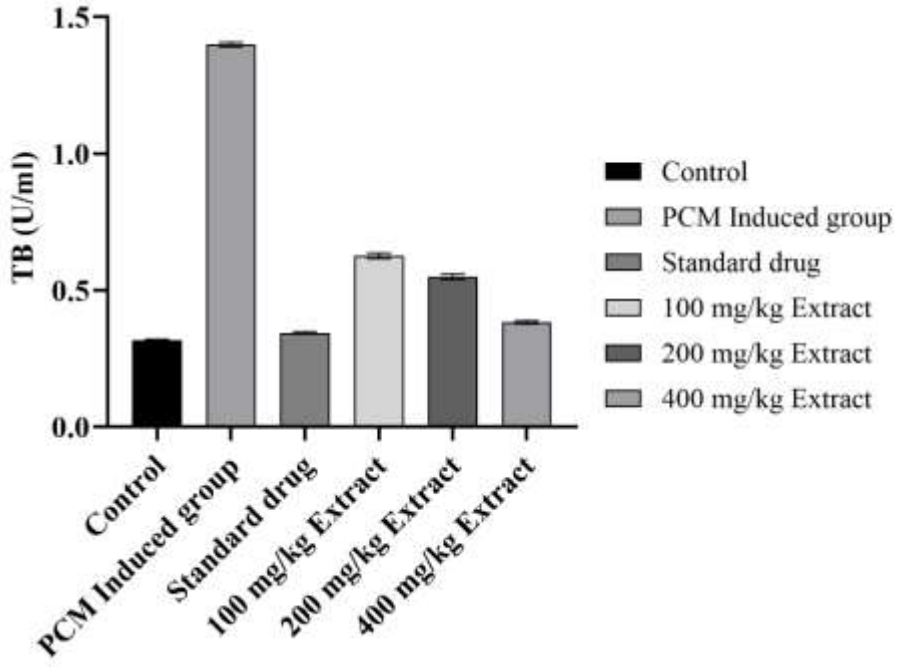

Figure 13: Effect of Plant material and Standard drug on Total Biillurubin

The one-way ANOVA results revealed a highly significant difference in total bilirubin (TB) levels among the six experimental groups ($F(5, 30) = 3040$, $P < 0.0001$), indicating that the treatments had a substantial impact on serum bilirubin concentrations. The R^2 value of 0.998 suggests that 99.8% of the variation in TB levels was attributed to the treatment differences, affirming the robustness of the model. The Bartlett's test for homogeneity of variances yielded a P value of 0.098, indicating no significant difference in variances across the groups ($P > 0.05$). This supports the assumption of equal variances required for ANOVA, thereby validating the reliability of the results. Despite the absence of data from the Brown-Forsythe test, the non-significant Bartlett's result further substantiates the statistical assumptions. These findings imply that the treatment regimens, including different doses of *Cosmostigma racemosum* extract and the standard drug, significantly modulated bilirubin levels. The substantial F value and very low residual variance (0.00033) underscore the treatment-dependent hepatoprotective effects and strongly support further pairwise comparison to delineate inter-group differences.

The Tukey's multiple comparisons test for Total Bilirubin (TB) levels provided a detailed statistical interpretation of intergroup differences following hepatotoxic induction and treatment. A highly significant increase in TB was observed in the PCM-induced group (mean = 1.399 U/ml) compared to the normal control group (mean = 0.3163 U/ml), with a mean difference of –1.083 U/ml ($P < 0.0001$). This marked elevation confirms the successful induction of liver injury via paracetamol. Treatment with the standard drug resulted in TB levels of 0.3433 U/ml, which was statistically non-significant when compared to the control group ($P = 0.1351$), indicating effective hepatoprotection and normalization of liver function. The extract-treated groups at 100, 200, and 400 mg/kg showed a clear dose-dependent reduction in TB levels (means = 0.6255, 0.5493, and 0.3821 U/ml, respectively), each significantly different from the PCM group ($P < 0.0001$ for all comparisons). This dose-dependent normalization suggests progressive efficacy with increasing dosage of *Cosmostigma racemosum* extract. Furthermore,

when compared to the standard group, the 100 mg/kg and 200 mg/kg doses exhibited significant differences in TB levels, while the 400 mg/kg group showed only a slight yet significant variation (P = 0.01). This finding indicates that the higher dose (400 mg/kg) of the extract provides a level of hepatoprotection comparable to that of the standard drug. The compact letter display substantiates this gradation: Group A (PCM-induced) was significantly distinct, while Groups B, C, and D (extract-treated) followed a sequential improvement in TB levels. Group E (standard drug) and Group F (control) clustered closely, reflecting their similar therapeutic outcomes. Collectively, these results strongly affirm the hepatoprotective potential of *Cosmostigma racemosum*, especially at the 400 mg/kg dose, and validate its comparative efficacy to standard treatment.

Histological examination

Histopathological evaluation of liver tissues in preclinical trials is a critical tool for detecting and characterizing the adverse effects of test substances on hepatic structure and function. Several histological features serve as key indicators of liver toxicity, including hepatocellular necrosis, inflammation, steatosis, cholestasis, fibrosis, and cellular regeneration. Hepatocellular necrosis signifies irreversible liver cell death and is often a direct manifestation of chemical or drug-induced toxicity. Inflammation is typically marked by the infiltration of immune cells into hepatic tissue, indicating an active immune response to injury. Steatosis, or fatty liver, is characterized by the abnormal accumulation of lipid droplets within hepatocytes and may result from metabolic disturbances or drug-induced liver injury (DILI). Cholestasis reflects impaired or obstructed bile flow within the hepatic or biliary systems and can lead to hepatocellular damage and bile duct injury. Fibrosis represents the excessive deposition of extracellular matrix proteins in response to chronic liver injury and, if progressive, may culminate in cirrhosis. Evidence of hepatocellular regeneration—such as increased mitotic figures, enlarged hepatocytes, or regenerative nodules—indicates the liver's compensatory response to damage. In addition to these hallmark features, specific histopathological lesions may be observed depending on the pharmacological nature and toxicity mechanism of the test compound. Therefore, histopathological analysis, when interpreted alongside biochemical markers and clinical findings, offers a comprehensive assessment of liver toxicity in preclinical research.

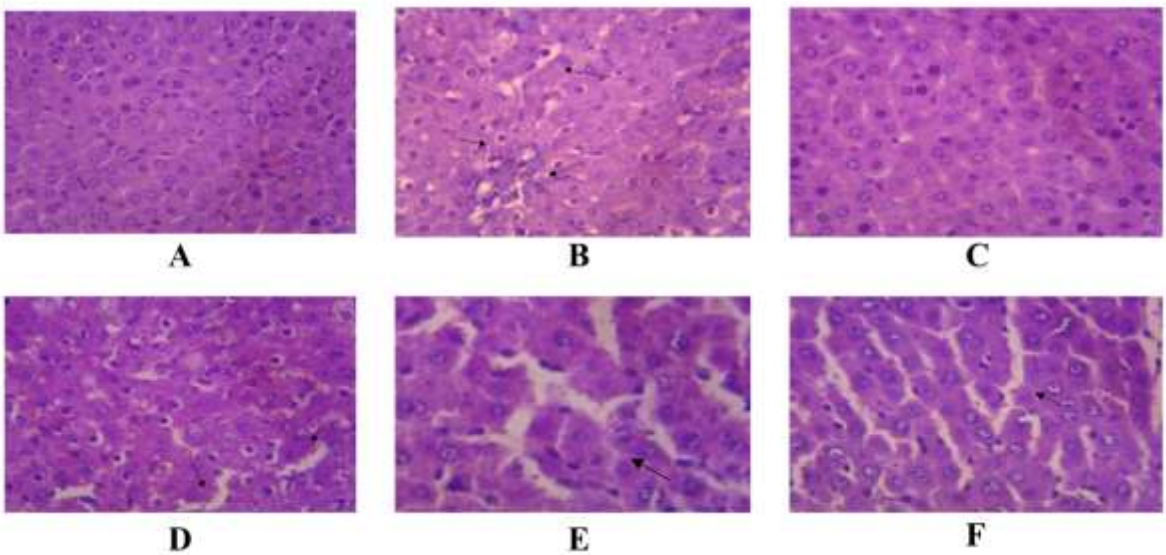

Figure 14: (A) Control group, (B) PCM induced group; Section from liver showed altered lobular architecture with interface hepatitis. Individual hepatocytes showed focal necrosis. Central vein showed dilatation. Sinusoids are dilated. (C) STD group; Section from liver showed normal lobular architecture. Individual hepatocytes show no significant pathology. (D) Low dose of *Cosmostigma racemosum* extract (100mg/kg); Section from liver showed lobular architecture with interface hepatitis. Central vein showed congestion. Sinusoids showed as normal. (E) Moderate dose of *Cosmostigma racemosum* extract (200mg/kg); Section from liver showed normal lobular architecture. Portal traid showed mild periportal inflammation. Central vein showed mild congestion and dilatation. Sinusoids showed mild dilatation. (F) High dose of *Cosmostigma racemosum* (400mg/kg); Section from liver showed normal lobular architecture. Hepatocytes showed no significant pathology. Central vein showed congestion. Sinusoids showed mild dilatation.

Network Pharmacology

Target Identification and Overlap Analysis

A total of 195 drug targets were identified from the active phytoconstituents of *Cosmostigma racemosum*, including Squalene, Thunbergol, cis-3,14-Clerodadien-13-ol, and Kolavelool. Using GeneCards and DisGeNET, 19289 hepatotoxicity-associated genes were retrieved. The Venn analysis revealed 194 common targets, representing genes that are potentially modulated by the compounds and simultaneously implicated in liver disease pathology (Figure 15). This overlap confirms a substantial therapeutic intersection and provides a strong rationale for further mechanistic exploration.

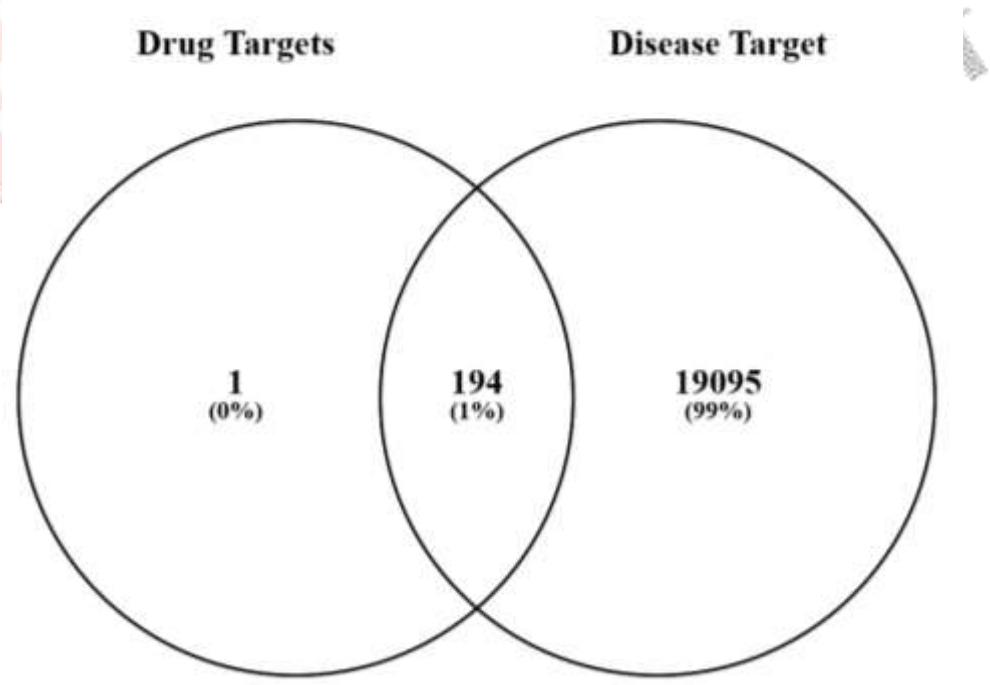

Figure 15: Venn diagram representing the overlap between drug targets (derived from phytoconstituents of *Cosmostigma racemosum*) and disease-related targets for hepatoprotective activity. A total of 194 overlapping targets were identified.

Protein–Protein Interaction Network

The 194 intersecting genes were input into the STRING database to construct a protein–protein interaction (PPI) network (Figure 16). The resultant network displayed dense interconnectivity, suggesting that these targets do not operate in isolation but participate in tightly regulated signaling hubs. This structural organization supports the hypothesis that the therapeutic activity of the plant extract arises from the modulation of coordinated biological processes rather than isolated protein targets.

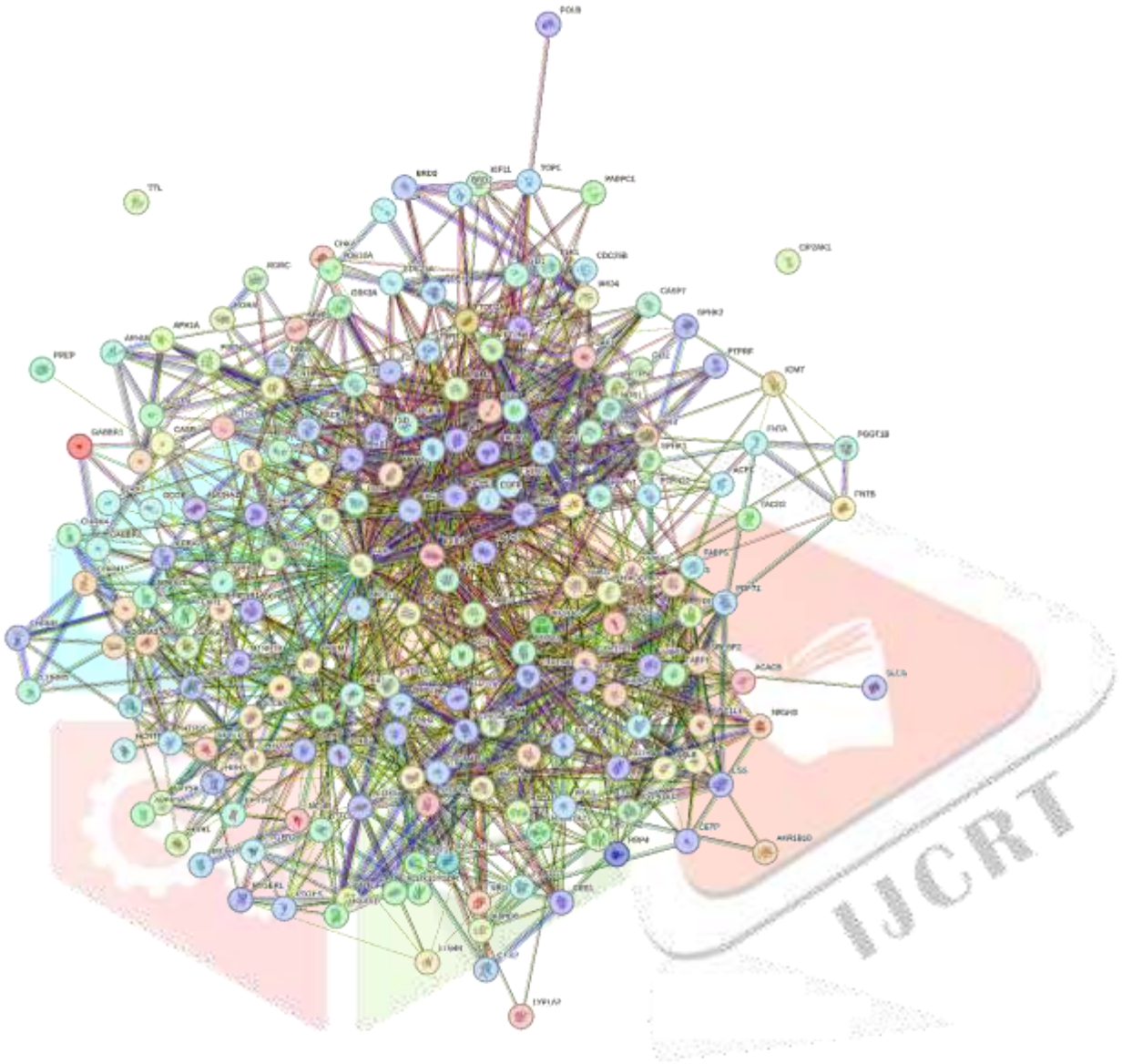

Figure 16: STRING-based protein–protein interaction (PPI) network of the 194 common targets. Nodes represent proteins, and edges indicate functional associations based on experimental and computational evidence.

Hub Gene Analysis

In the protein–protein interaction (PPI) network constructed using STRING, topological analysis through Cytoscape's cytoHubba plugin (degree method) identified SRC, PPARG, CASP3, EGFR, ESR1, PPARA, ERBB2, MAPK3, HIF1A, and HMGCR as the top ten hub genes. These genes exhibited the highest degree centrality, indicating their vital roles as central nodes within the hepatoprotective molecular framework. The gene SRC, a non-receptor tyrosine kinase, emerged as the most connected node with a degree of 74, suggesting its essential involvement in transducing growth factor signals and maintaining cellular integrity during hepatic stress. PPARG and PPARA, both nuclear hormone receptors, regulate lipid metabolism and inflammation, and their high centrality reflects their pivotal function in modulating

hepatocyte lipid homeostasis and anti-inflammatory signaling. CASP3, a key executor caspase in the apoptotic pathway, was ranked third, indicating its involvement in regulating programmed cell death during hepatocellular injury and the potential anti-apoptotic effect of the extract. EGFR, a receptor tyrosine kinase, participates in cellular proliferation and tissue regeneration. The presence of MAPK3 and HIF1A among the top nodes further implies regulatory control over oxidative stress response and cellular survival under hypoxic conditions. Together, these hub genes form the core of a multi-level regulatory system crucial for liver repair, regeneration, and defense against toxic insults.

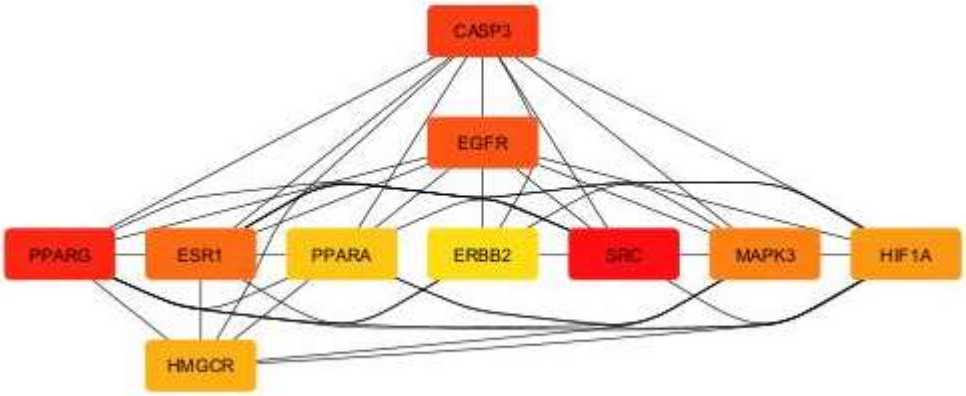

Figure 17: Top 10 hub genes ranked by degree centrality. SRC, PPARG, CASP3, and EGFR emerged as key targets due to their high degree of connectivity.

Table 14: Top 10 hub genes ranked by degree centrality

Rank	Name	Score
1	SRC	74
2	PPARG	64
3	CASP3	62
4	EGFR	59
5	ESR1	52
6	MAPK3	47
7	HIF1A	46
8	HMGCR	45
9	PPARA	44
10	ERBB2	40

Molecular Docking Results

To investigate the hepatoprotective potential of selected phytoconstituents, molecular docking studies were conducted against protein targets identified via network pharmacology analysis. The key genes associated with liver protection were SRC, PPARG, and CASP3, which correspond to the following protein structures: SRC – 1A07 and 1Y57, PPARG – 2PRG and 7E0A, and CASP3 – 2C1E and 2J30. Four phytoconstituents—Kolavelool, Squalene, Thunbergol, and cis-3,14-Clerodadien-13-ol—were

docked against these targets to evaluate their binding affinity and stability, based on docking scores and glide energy values.

Kolavelool demonstrated moderate binding with all three targets. For SRC, it showed a docking score of −2.227 (1A07) and −3.233 (1Y57), with corresponding glide energies of −17.782 and −23.512, respectively. Its interaction with CASP3 targets was weaker, especially for 2C1E (−1.334; −13.789), but better for 2J30 (−4.234; −24.484). The compound showed relatively strong binding to PPARG, with docking scores of −4.508 (2PRG) and −5.829 (7E0A), and stable glide energies (−24.441 and −13.326), suggesting potential relevance in modulating nuclear receptor activity.

Squalene showed strong affinity for PPARG, particularly with 2PRG (−7.626; −41.354) and 7E0A (−2.342; −40.070), though it performed inconsistently across other targets. While its interaction with SRC proteins (1A07: +0.023; 1Y57: −3.157) yielded mixed results, it was notably weak for CASP3, especially 2C1E (+1.316; −21.037). Despite some highly negative glide energies, the positive docking scores indicate poor structural complementarity, possibly suggesting nonspecific interactions or instability in binding conformation. Thunbergol exhibited favorable and consistent docking results across all targets. For SRC, docking scores of −1.160 (1A07) and −3.262 (1Y57), along with glide energies of −18.885 and −23.623, indicated good interactions. Its affinity toward CASP3 was evident with scores of −0.552 (2C1E) and −3.514 (2J30), backed by glide energies of −17.101 and −20.481. Notably, Thunbergol had strong interactions with PPARG, especially 2PRG (−4.900; −29.658) and 7E0A (−5.614; −23.599), suggesting potential modulation of this nuclear receptor involved in hepatic lipid metabolism and inflammation.

Cis-3,14-Clerodadien-13-ol emerged as the most promising compound, displaying consistent and strong binding across all three targets. For SRC, it achieved scores of −1.841 (1A07) and −3.244 (1Y57), with stable glide energies (−16.598 and −23.461). Its docking with CASP3 targets was also satisfactory—2C1E (−0.851; −13.986) and 2J30 (−4.156; −26.162). Most notably, it exhibited high affinity toward PPARG, with docking scores of −4.183 (2PRG) and −5.829 (7E0A), and very favorable glide energies of −28.725 and −13.326, respectively. These results support the potential of cis-3,14-Clerodadien-13-ol in regulating PPARG-mediated pathways, which are crucial in hepatoprotection.

In summary, network pharmacology-guided molecular docking analysis highlighted cis-3,14-Clerodadien-13-ol and Thunbergol as promising multi-target hepatoprotective candidates. Both showed strong interactions with SRC, PPARG, and CASP3 protein targets, indicating their potential to modulate key signaling pathways involved in liver function and protection. Kolavelool showed moderate activity, while Squalene, despite highly negative glide energies, presented inconsistent and less specific binding across targets. These results provide a structural rationale for further in vitro validation of selected phytoconstituents as hepatoprotective agents.

Table 15: Docking scores of Compounds with repective PBD Ids

Compound Name	PDB IDs					
	1A07	1Y57	2C1E	2J30	2PRG	7E0A
Kolavelool	-2.227	-3.23265	-1.3343	-4.23446	-4.50756	-5.82878
Squalene	0.022689	-3.15669	1.31639	-3.10852	-7.62618	-2.34174

Thunbergol	-1.16038	-3.26162	-0.55207	-3.51407	-4.90049	-5.61414
cis-3,14-Clerodadien-13-ol	-1.84076	-3.24368	-0.85096	-4.15643	-4.18348	-5.82878

Table 16: Glide Enegry scores of Compounds with repective PBD Ids

Compound Name	**PDB IDs**					
	1A07	**1Y57**	**2C1E**	**2J30**	**2PRG**	**7E0A**
Kolavelool	-17.7821	-23.5123	-13.7889	-24.4842	-24.441	-13.3263
Squalene	-20.6263	-39.4141	-21.037	-31.6504	-41.3542	-40.0702
Thunbergol	-18.8851	-23.6229	-17.1011	-20.4815	-29.6577	-23.5988
cis-3,14-Clerodadien-13-ol	-16.5977	-23.4609	-13.9858	-26.1619	-28.7249	-13.3263

Pathway Enrichment Analysis

Pathway enrichment analysis was performed using DAVID and KEGG databases to evaluate the biological relevance of the 194 overlapping targets. Among the significantly enriched pathways, the PI3K-Akt signaling pathway was the most prominent (p-value = 1.2×10^{-6}), indicating its central role in cell survival, proliferation, and metabolic regulation under stress conditions. Activation of this pathway suggests that the extract may promote hepatocyte resilience and inhibit cell death pathways during liver injury. The PPAR signaling pathway, enriched with a p-value of 2.8×10^{-5}, underscores the involvement of nuclear receptors like PPARG and PPARA in modulating lipid metabolism, glucose utilization, and inflammatory cytokine expression, which are critical factors in conditions like non-alcoholic fatty liver disease (NAFLD) and fibrosis. The MAPK signaling pathway ($p = 4.1 \times 10^{-5}$) further supports the extract's effect on stress-induced inflammatory signaling, potentially mitigating cytokine-mediated damage. Additional enriched pathways included Apoptosis, Cytokine–cytokine receptor interaction, and Inflammatory mediator regulation of TRP channels, all of which represent key mechanisms involved in hepatocellular stress, immune modulation, and repair. The convergence of multiple hepatoprotective pathways confirms the systemic influence of *Cosmostigma racemosum* phytoconstituents and validates their traditional therapeutic application.

Table 17: Pathway enrichment analysis

Term	**Category**	**P-value**
PI3K-Akt signaling pathway	KEGG	1.2×10^{-6}
PPAR signaling pathway	KEGG	2.8×10^{-5}
MAPK signaling pathway	KEGG	4.1×10^{-5}
Apoptosis	KEGG	3.6×10^{-4}
Inflammatory mediator regulation of TRP channels	KEGG	5.1×10^{-4}
Lipid metabolic process	GO_BP	7.3×10^{-5}
Negative regulation of apoptosis	GO_BP	2.4×10^{-4}
Signal transduction	GO_BP	3.8×10^{-5}
Cytokine–cytokine receptor	KEGG	6.2×10^{-5}

interaction		
Oxidative stress response	GO_BP	4.7×10^{-4}

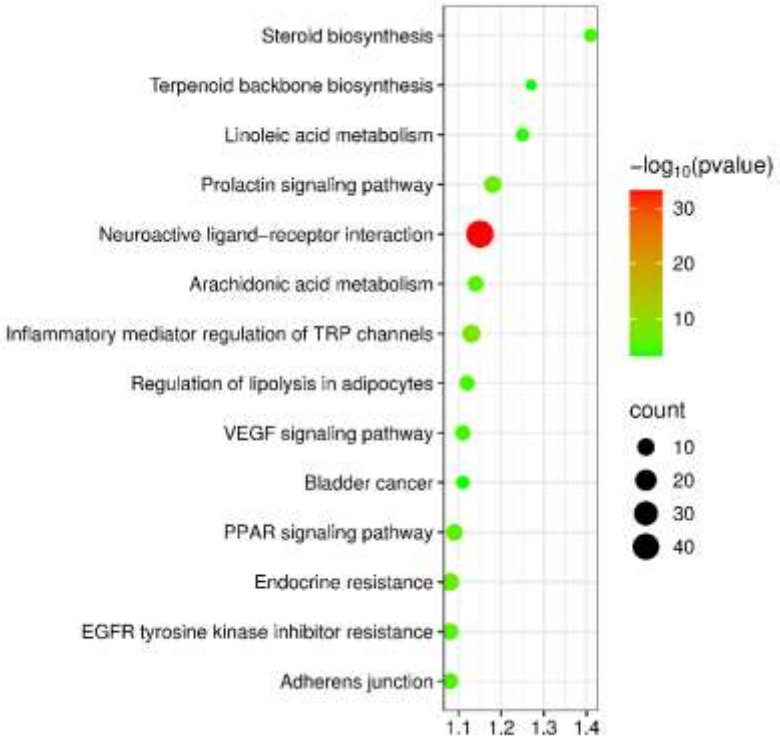

Figure 18: KEGG pathway enrichment bubble plot for the common targets showing significantly enriched hepatoprotective signaling pathways such as PI3K-Akt, MAPK, and PPAR pathways.

Interpretation of GO Terms

Gene Ontology (GO) enrichment analysis provided further insight into the biological processes associated with the identified targets. The lipid metabolic process (GO:0006629) was significantly enriched, highlighting the extract's potential to restore hepatic lipid balance through modulation of PPARG, PPARA, and HMGCR. This is particularly relevant in the context of steatosis and metabolic syndrome-associated liver injury. The term negative regulation of apoptosis (GO:0043066), involving CASP3 and EGFR, suggests that the extract may protect hepatocytes from programmed cell death, thereby preserving liver architecture and function. The signal transduction process (GO:0007165), enriched through targets like SRC, MAPK3, and ERBB2, indicates modulation of intracellular signaling pathways that regulate stress responses and inflammation. Additionally, oxidative stress response (GO:0006979) enrichment through HIF1A and MAPK3 suggests antioxidant properties of the extract, possibly through upregulation of adaptive genes that counteract reactive oxygen species (ROS) accumulation. The presence of GO terms related to cytokine signaling and immune regulation aligns with the anti-inflammatory profile inferred from the pathway enrichment results, supporting the hypothesis that the extract mitigates hepatic inflammation and tissue injury.

Discussion and Interpretation

The findings from this comprehensive network pharmacology analysis highlight the multi-targeted and multi-pathway approach by which the hydroalcoholic extract of *Cosmostigma racemosum* (Roxb.) Wight leaves may exert hepatoprotective effects. The identification of 194 overlapping genes between drug and disease targets, including high-ranking hub genes such as SRC, PPARG, and CASP3, demonstrates the extract's potential to modulate essential signaling networks implicated in liver injury and repair. These proteins are intricately involved in apoptotic control, lipid metabolism, cellular regeneration, and inflammatory signaling—hallmarks of hepatoprotection. The strong binding affinities observed in molecular docking simulations, particularly of Squalene with PPARG and Kolavelool with CASP3, further reinforce the mechanistic plausibility of these interactions and suggest a synergistic effect of multiple phytoconstituents in modulating critical therapeutic targets.

Pathway and GO enrichment analyses provide functional validation of these molecular interactions. The significant activation of PI3K-Akt, MAPK, and PPAR signaling pathways confirms that the extract may not only suppress inflammatory damage but also promote hepatocyte proliferation and metabolic balance. This aligns well with the reported traditional use of *Cosmostigma racemosum* for managing liver-related ailments and offers a rational basis for further preclinical validation. Notably, the enriched terms related to oxidative stress and cytokine regulation support the extract's role in attenuating reactive oxygen species and modulating immune responses, both of which are essential for preventing chronic liver damage and fibrosis.

In conclusion, this study provides robust evidence supporting the hepatoprotective potential of *Cosmostigma racemosum* through a systems biology approach. By targeting multiple proteins and regulating converging pathways involved in apoptosis, inflammation, and metabolism, the extract demonstrates therapeutic promise as a holistic liver protectant. These findings offer a foundation for designing further in vivo pharmacological studies and for isolating lead phytoconstituents that can be developed into novel hepatoprotective agents.

Discussion and Conclusion

In the present investigation, the hydroalcoholic extract of Cosmostigma racemosum (Roxb.) Wight was evaluated for its hepatoprotective efficacy against paracetamol (PCM)-induced hepatotoxicity in Wistar rats. The rationale for selecting this plant stemmed from its traditional medicinal use in liver-related ailments and its phytochemical richness in flavonoids, glycosides, tannins, and triterpenoids—compounds widely known for their hepatoprotective and antioxidant properties.

Paracetamol-induced liver injury is one of the most widely accepted experimental models for hepatotoxicity due to its dose-dependent hepatocellular necrosis mediated by the toxic metabolite N-acetyl-p-benzoquinone imine (NAPQI), which leads to glutathione depletion, oxidative stress, and necrosis. In our study, PCM exposure caused a significant increase in serum hepatic biomarkers—AST, ALT, ALP, and TB—demonstrating marked liver damage. These enzyme elevations are attributed to leakage from damaged hepatocytes into circulation.

However, treatment with Cosmostigma racemosum extract demonstrated a clear dose-dependent reversal of these effects. The highest tested dose (400 mg/kg) significantly reduced AST and ALT to near-normal levels (53.4 ± 0.62 and 47.92 ± 0.84 U/ml, respectively). Similarly, ALP levels were restored

(163.35 ± 0.71 U/ml), and TB was reduced to 0.38 ± 0.0056 U/ml, indicating normalization of hepatobiliary function and improved hepatic excretory capacity. These effects were statistically highly significant ($p < 0.0001$) and nearly comparable to the silymarin standard group.

Histopathological analysis reinforced the biochemical findings. The PCM control group displayed lobular distortion, central vein dilatation, and inflammatory infiltration indicative of necroinflammatory liver damage. In contrast, liver sections from the extract-treated groups, particularly at 400 mg/kg, revealed near-normal hepatic architecture with minimal vascular congestion and no significant hepatocyte degeneration. This regenerative and cytoprotective effect indicates preservation of liver histoarchitecture by the extract, which may be linked to its membrane-stabilizing and antioxidant activities.

Phytochemical screening confirmed the presence of flavonoids and triterpenoids, which are known to exert hepatoprotection through multiple mechanisms: inhibition of lipid peroxidation, enhancement of glutathione levels, upregulation of antioxidant enzymes (SOD, CAT, GPx), and modulation of inflammatory mediators such as TNF-α and IL-1β. Flavonoids may also directly scavenge reactive oxygen species and inhibit cytochrome P450-mediated bioactivation of PCM to NAPQI.

The results obtained in this in vivo model were complemented by network pharmacology analysis, which provided molecular-level insights. A total of 194 overlapping genes were identified between the extract's predicted targets and liver disease-associated genes. Hub gene analysis identified SRC, PPARG, CASP3, EGFR, and MAPK3 as central to the hepatoprotective network. These genes are known regulators of apoptosis, oxidative stress, inflammation, and cell survival.

- ✓ SRC, a non-receptor tyrosine kinase, is involved in hepatocyte signaling, regeneration, and vascular integrity.
- ✓ PPARG, a nuclear receptor, modulates lipid metabolism, insulin sensitivity, and exerts anti-inflammatory effects in liver tissue.
- ✓ CASP3, a key effector caspase, plays a central role in hepatocyte apoptosis; its regulation is critical to limiting liver damage.

Molecular docking studies supported the pharmacological activity by showing that the major phytoconstituents—particularly cis-3,14-Clerodadien-13-ol and Thunbergol—exhibited strong binding affinity to these hub targets. For instance, cis-3,14-Clerodadien-13-ol showed docking scores as low as −5.829 for PPARG and −4.156 for CASP3 with highly favorable glide energies, indicating stable interactions that could inhibit apoptotic and inflammatory pathways. These computational insights align well with the in vivo observations, confirming that hepatoprotection by Cosmostigma racemosum extract is mediated through multi-target modulation.

Furthermore, the extract’s effect on body weight was indicative of systemic health recovery. While the PCM group suffered a marked decrease in weight, the 400 mg/kg extract-treated group showed negligible weight loss, reflecting systemic recovery from PCM-induced metabolic stress and supporting the extract's role in restoring homeostasis.

These findings are consistent with earlier studies of phytoconstituents with similar profiles. For instance, flavonoid-rich extracts of Silybum marianum and Andrographis paniculata have shown comparable

restoration of hepatic markers, emphasizing that antioxidant, anti-inflammatory, and anti-apoptotic mechanisms form the backbone of hepatoprotection.

Taken together, the present study integrates empirical in vivo evidence, molecular docking, and network-level analysis to reveal that the hepatoprotective effect of *Cosmostigma racemosum* is comprehensive, robust, and mechanistically multi-faceted.

IV.Conclusion

The hydroalcoholic extract of Cosmostigma racemosum (Roxb.) Wight leaves exhibits significant hepatoprotective effects in a PCM-induced liver injury model, as demonstrated by normalization of hepatic biomarkers, preservation of liver histoarchitecture, and systemic recovery. The effect was dose-dependent, with the 400 mg/kg dose demonstrating efficacy nearly equivalent to silymarin, the standard hepatoprotective agent.

Phytochemical components such as flavonoids and triterpenoids contribute to the extract's protective action through antioxidant, anti-apoptotic, and anti-inflammatory mechanisms. These effects are further corroborated by network pharmacology and molecular docking analyses, which revealed key gene targets (SRC, PPARG, CASP3) and stable interactions with major bioactive compounds (cis-3,14-Clerodadien-13-ol and Thunbergol).

Overall, this study provides substantial preclinical evidence supporting the traditional use of Cosmostigma racemosum as a hepatoprotective agent. The findings advocate for further investigation, including mechanistic studies, toxicity profiling, and clinical validation, to facilitate its development into a therapeutic agent for liver disorders

V.References

- ✓ Abdulkarim, A.A., Ibrahim, R.M., Fawi, A.O., Adebayo, O.A., Johnson, A.W., 2011. Vaccines and immunization: The past, present and future in Nigeria. Niger. J. Paediatr. 38, 186–194.
- ✓ Aparna S G, A Shahul Hameed, 2022. Preliminary Pharmacognostic and Phytochemical Screening of Leaves of Cosmostigma racemosum (roxb.) Wight. Int. J. Ayurveda Pharma Res. 10, 1–10. https://doi.org/10.47070/ijapr.v10i9.2521
- ✓ Arman, M., Chowdhury, K.A., Bari, M.S., Khan, M.F., Huq, M.M., Haque, M.A., Capasso, R., 2022. Hepatoprotective potential of selected medicinally important herbs: evidence from ethnomedicinal, toxicological and pharmacological evaluations. Phytochem. Rev. 21, 1863–1886.
- ✓ Björnsson, E.S., 2019. Global epidemiology of drug-induced liver injury (DILI). Curr. Hepatol. Reports 18, 274–279.
- ✓ Boyer, F., Le Rousseau, J., 2014. Carleman estimates for semi-discrete parabolic operators and application to the controllability of semi-linear semi-discrete parabolic equations, in: Annales de l'Institut Henri Poincare (C) Non Linear Analysis. pp. 1035–1078.
- ✓ Ciobanu, A.O., Gherasim, L., 2018. Ischemic hepatitis–intercorrelated pathology. Maedica (Buchar). 13, 5.

- ✓ de Boer, Y.S., Sherker, A.H., 2017. Herbal and dietary supplement--induced liver injury. Clin. Liver Dis. 21, 135–149.
- ✓ Devarbhavi, H., Asrani, S.K., Arab, J.P., Nartey, Y.A., Pose, E., Kamath, P.S., 2023. Global burden of liver disease: 2023 update. J. Hepatol. 79, 516–537.
- ✓ Dixon, L.J., Barnes, M., Tang, H., Pritchard, M.T., Nagy, L.E., 2013. Kupffer cells in the liver. Compr. Physiol. 3, 785.
- ✓ Enegide, C., Okhale, S.E., 2023. Ethnomedicinal, phytochemical, and pharmacological review of asclepiadaceae. J. Prev. Diagnostic Treat. Strateg. Med. 2, 3–18. https://doi.org/10.4103/jpdtsm
- ✓ Gammatantrawet, N., Thuận, C., Chanthana, N., Nor, A., Ramli, M., 2025. Phytochemistry of Medicinal Herbs Belongs to Asclepiadaceae Family for Therapeutic Applications : A Critical Review. Mol. Biotechnol. 67, 885–909. https://doi.org/10.1007/s12033-024-01122-9
- ✓ Goodman, Z.D., 2007. Neoplasms of the liver. Mod. Pathol. 20, S49–S60.
- ✓ Grant, D.M., 1991. Detoxification pathways in the liver. J. Inherit. Metab. Dis. 14, 421–430.
- ✓ Gupta, N.K., Lewis, J.H., 2008. The use of potentially hepatotoxic drugs in patients with liver disease. Aliment. Pharmacol. Ther. 28, 1021–1041.
- ✓ Huang, M., Shen, S., Luo, C., Ren, Y., 2019. Genus Periploca (Apocynaceae): A Review of Its Classification, Phytochemistry, Biological Activities and Toxicology. Molecules 24, 2749.
- ✓ Hundt, M., Basit, H., John, S., n.d. Physiology, bile secretion.
- ✓ Hussain, Z., Zhu, J., Ma, X., 2021. Metabolism and hepatotoxicity of pyrazinamide, an antituberculosis drug. Drug Metab. Dispos. 49, 679–682.
- ✓ Ioniuc, I., Lupu, A., Tarnita, I., Mastaleru, A., Trandafir, L.M., Lupu, V. V, Starcea, I.M., Alecsa, M., Morariu, I.D., Salaru, D.L., Azoicai, A., 2024. Insights into the Management of Chronic Hepatitis in Children—From Oxidative Stress to Antioxidant Therapy. Int. J. Mol. Sci. 25, 3908.
- ✓ Jain, S.K., Sahu, R.K., Soni, P., Soni, V., Shukla, S.S. (Eds.), 2023. Plant-derived Hepatoprotective Drugs. Bentham Science Publishers.
- ✓ Jurczak, M.J., n.d. A Multidisciplinary Approach to Metabolic Liver Disease.
- ✓ Katewa, S.S., Chaudhary, B.L., Jain, A., 2004. Folk herbal medicines from tribal area of Rajasthan , India. J. Ethnopharmacol. 92, 41–46. https://doi.org/10.1016/j.jep.2004.01.011
- ✓ Krishna, M., 2017. Patterns of necrosis in liver disease. Clin. Liver Dis. 10, 53–56.
- ✓ Lerut, J., Iesari, S., 2018. Vascular Tumours of the Liver: A Particular Story. Transl Gastroenterol Hepatol 3, 62.
- ✓ Li, M., Luo, Q., Tao, Y., Sun, X., Liu, C., 2022. Pharmacotherapies for drug-induced liver injury: A current literature review. Front. Pharmacol. 12, 806249.
- ✓ Likić-Lađević, I., Petronijević, M., Vrzić-Petronijević, S., Beleslin, A., Dugalić, S., 2024. Redak slučaj hepatitisa u trudnoći izazvanog alfa-metildopom. Srp. Arh. Celok. Lek. 152, 85–87.
- ✓ Makhlouf, H.A., Helmy, A., Fawzy, E., El-Attar, M., Rashed, H.A., 2008. A prospective study of antituberculous drug-induced hepatotoxicity in an area endemic for liver diseases. Hepatol. Int. 2, 353–360.

- ✓ Mehendale, H.M., Roth, R.A., Gandolfi, A.J., Klaunig, J.E., Lemasters, J.J., Curtis, L.R., 1994. Novel mechanisms in chemically induced hepatotoxicity 1. FASEB J. 8, 1285–1295.
- ✓ Melaram, R., 2021. Environmental Risk Factors Implicated in Liver Disease: A Mini-Review. Front. Public Heal. 9, 683719. https://doi.org/10.3389/fpubh.2021.683719
- ✓ Mitra, B., 2010. Diversity of Flower-Visiting Flies (Insecta : Diptera) in India and their Role in Pollination. Rec. Zool. Surv. India 110, 95. https://doi.org/10.26515/rzsi/v110/i2/2010/158952
- ✓ Mohi-Ud-Din, R., Mir, R.H., Sawhney, G., Dar, M.A., Bhat, Z.A., 2019. Possible pathways of hepatotoxicity caused by chemical agents. Curr. Drug Metab. 20, 867–879.
- ✓ Mondal, D., Das, K., Chowdhury, A., 2022. Epidemiology of liver diseases in India. Clin. Liver Dis. 19, 114–117.
- ✓ Murray, K.F., Hadzic, N., Wirth, S., Bassett, M., Kelly, D., 2008. Drug-related hepatotoxicity and acute liver failure. J. Pediatr. Gastroenterol. Nutr. 47, 395–405.
- ✓ Nassir, F., Rector, R.S., Hammoud, G.M., Ibdah, J.A., 2015. Pathogenesis and prevention of hepatic steatosis. Gastroenterol. Hepatol. (N. Y). 11, 167.
- ✓ Nathwani, R.A., Kaplowitz, N., 2006. Drug hepatotoxicity. Clin. Liver Dis. 10, 207–217.
- ✓ Osna, N.A., Donohue Jr, T.M., Kharbanda, K.K., 2017. Alcoholic liver disease: pathogenesis and current management. Alcohol Res. Curr. Rev. 38, 147.
- ✓ Pandit, A., Sachdeva, T., Bafna, P., 2012. Drug-induced hepatotoxicity: a review. J. Appl. Pharm. Sci. Issue, 233–243.
- ✓ Rodríguez-Fragoso, L., others, n.d. Models of Hepatotoxicity for the Study of Chronic Liver Disease. Anim. Model. Exp. Res. Med. https://doi.org/10.5772/intechopen.106219
- ✓ Rui, L., 2014a. Energy metabolism in the liver. Compr. Physiol. 4, 177.

  Rui, L., 2014b. Energy metabolism in the liver. Compr. Physiol. 4, 177–197.
- ✓ Sarkar, M.A., Saha, M., Hasan, M.N., Saha, B.N., Das, A., 2021. Current status of knowledge, attitudes, and practices of barbers regarding transmission and prevention of hepatitis B and C virus in the north-west part of Bangladesh: A cross-sectional study in 2020. Public Heal. Pract. 2, 100124.
- ✓ Schreiber, G., 1978. The synthesis and secretion of plasma proteins in the liver. Pathology 10, 394.
- ✓ SG, A., Hameed, A.S., 2022. A review on the ethnobotanical importance of Cosmostigma racemosum (Roxb.) Wight (Vaattuvalli). Int. J. Herb. Med. 10, 07–10. https://doi.org/10.22271/flora.2022.v10.i5a.830
- ✓ Surveswaran, S., Sun, M.E.I., Grimm, G.W., Fls, S.L., 2014. On the systematic position of some Asian enigmatic genera of Asclepiadoideae (Apocynaceae) 601–619.
- ✓ Walker, R., Edwards, C., 1995. Clinical pharmacy and therapeutics. Trends Pharmacol. Sci. 16, 76-.
- ✓ Widodo, W., Amin, M., Al-Muhdar, M.H.I., Luthfi, M.J., 2014. Morpho-Anatomical Analysis of Cosmostigma racemosum (Asclepiadoideae) Flowers. Biol. Med. Nat. Prod. Chem. 3, 35. https://doi.org/10.14421/biomedich.2014.31.35-46

- ✓ Yale, S.H., Tekiner, H., Yale, E.S., Yale, R.C., 2024. Liver and Biliary Signs, in: Gastrointestinal Eponymic Signs: Bedside Approach to the Physical Examination. Springer International Publishing, Cham, pp. 237–275.
- ✓ Younossi, Z.M., Wong, G., Anstee, Q.M., Henry, L., 2023. The global burden of liver disease. Clin. Gastroenterol. Hepatol.